AIR FORCE 

INSTITUTE OF TECHNOLOGY

AIR UNIVERSITY

RESIDENT COLLEGE

WRIGHT-PATTERSON AIR FORCE BASE-OHIO

ATTAINMENT OF NEUTRON FLUX-SPECTRA FROM FOIL ACTIVATIONS

THESIS

Presented to the Faculty of the School of Engineering of
the Air Force Institute of Technology
Air University
in Partial Fulfillment of the
Requirement for the Degree of
Master of Science

By
Paul Michael Uthe, Jr., B.S.E.P.
1/Lt U.S.A.F.
Graduate Nuclear Engineering

March 1957

Preface

It is the purpose of this thesis to describe several methods of obtaining neutron flux-spectra information from foil data. These methods, although presented in considerable detail, are not yet in optimized form. It is hoped that this can be done in the near future.

It is well known that threshold and fission type foils are most advantageously used to generate integral flux data. Since radiation effects investigators usually desire dose parameters rather than flux parameters, a method of calculating the dose from integral flux data is presented in Appendix A.

The author wishes to thank Dr. W. J. Price and Lt. Col. B. E. Robertson for their helpful advice and consideration. The author is greatly indebted to Lt. W. R. Burrus, Materials Laboratory, for his many pertinent suggestions and comments. Dr. M. A. Edwards, Lt. T. A. Brown, and their associates of the Computations Branch, Aeronautical Research Laboratory, suggested some of the mathematical techniques and handled the programming of the digital computer. Mr. S. A. Szawlewicz, Materials Laboratory, gratiously made the necessary financial arrangements for the computer program. Without the ideas and assistance of any of the above mentioned people, this thesis would not have been possible.

Paul M. Uthe, Jr.

Contents

List of Figures

List of Tables

Abstract

Several analytical methods are described for obtaining neutron flux-spectra knowledge from foil data. The response functions used are the nuclear reaction characteristics of threshold, fast fission, and resonance type foils.

Two previously used methods and two new methods are discussed. The previously used methods are the Trice Method and the Cadmium Difference Method. The Trice Method, applicable in the fast neutron energy region, uses a "step function" cross section representation. The step function energy threshold is determined by assuming a differential flux function. The Cadmium Difference Method, applicable in the 1/E energy region, uses the resonance activation integrals of resonance type foils as cross section parameters. Although consideration is given to these methods, major interest is focused on two new methods. These methods are called the Polygonal Method and the Polynomial Method.

The Polygonal Method uses the cross sections in their true form and represents the flux-energy spectrum by a combination of linear functions of energy. In performing the necessary calculations, difficulty in selecting certain energy parameters is experienced.

The Polynomial Method uses the cross sections in their true form and represents the flux-energy spectrum by a weighting function

times a polynomial. The degree of the polynomial is one less than the number of different foils used. A digital computer is conveniently used for the required numerical calculations.

The result of several test cases using the Polynomial Method indicates that considerable improvement over the Trice Method is achieved.

GNE-9

ATTAINMENT OF NEUTRON FLUX-SPECTRA FROM FOIL ACTIVATIONS

I. Introduction

The purpose of this thesis is to describe several methods for obtaining neutron-flux spectra* in high intensity reactors. Knowledge of the neutron flux environment is required for the effective interpretation of the results obtained from radiation effects experiments. The analysis methods described are designated as:

A. The Trice Method

B. The Cadmium Difference Method

C. The Polygonal Method

D. The Polynomial Method

These methods are presented in Sections 3, 5, and 6 respectively.

The analysis methods are based upon the nuclear reaction characteristics of three types of foils: (1) threshold, (2) fast fission, and (3) resonance. The word "foil" does not imply a physical characteristic; i.e., a foil may be in powder, pellet, liquid or other

* In the remainder of this report, "spectra" signifies "energy spectra."

physical form. The word "radioactivant", though not commonly used, would be more appropriate.

Major interest is focused on the threshold and fast-fission types of foils. For the sake of generalty, some brief comments regarding resonance type foils are included. It is believed, however, that the calculational methods derived are sufficiently general so as to be applicable to any detector system.

Of the many techniques that have been used to determine reactor neutron spectra, the foil technique is the most often used. This is so, not because the foil gives the most precise information, but because it has the greatest compatibility with the nuclear and physical reactor characteristics. Three specific reasons for this general acceptance are as follows: (1) only a few milligrams of foil are needed in most cases; (2) the foil, with suitable cover, is the complete detector; and (3) all analysis is done in a convenient nuclear counting room after irradiation. It is not surprising that the radioactivant foil has achieved such popularity in this era of large and complicated experiments.

On the other hand, the use of foils does introduce several complications. Extreme care must be taken in the processing of the foils (both before and after irradiation). If this is not done, misleading results may be obtained. In the end, the proper use of foils reduces to an art rather than a science, for once the correct

irradiation and counting data are recorded, spectral information can be generated from the original data as better analytical methods become available. In this study, analytical methods will be emphasized. As of this writing, the methods have not been subjected to a good test or intercomparison; however, it is hoped that this can be done in the near future.

II. Characteristics of Foils

General

Before the analytical methods can be discussed, it is necessary to discuss the nuclear characteristics of certain types of foils. This is necessary because the usefulness of the analysis methods is directly dependent upon the neutron reaction characteristics of certain types of foils.

In general, when materials are irradiated in a neutron flux, neutron induced transmutation of their nuclei may occur. As an example, neutron-gamma (n,γ), neutron-proton (n,p), and neutron-alpha (n,α) reactions occur in aluminum-27 when this material is irradiated in a nuclear reactor. Each of these reactions leads to a new and different isotope, each isotope being radioactive. It is the radioactive decay of the isotopes which is observed in the counting room.

The reaction probabilities or cross sections are functions of neutron energy. It is the unusual nature of the reaction cross sections of several materials which is responsible for their usefulness as neutron flux-spectra detectors.

The number of particular transmutations occurring in a unit interval of time, per unit volume of material, due to neutrons having energies in the energy range dE about E is:

$$R(E)\,dE = \phi(E)\ \sigma_i(E)\ N\,dE \qquad (1)$$

$$\frac{R(E)}{N}\,dE = \phi(E)\ \sigma_i(E)\,dE \qquad (2)$$

Where: $R(E)\,dE$ = the number of transmutations per cc per sec due to neutrons in the energy range dE about E.

$\phi(E)$ = the differential neutron flux in neutrons per cm^2 per sec per energy interval.

$N\sigma_i(E)$ = the probability of the ith type of transmutation occurring per unit distance of travel of a neutron with energy E.

N = the number of pertinent isotopic nuclei per cc.

$\sigma_i(E)$ = the microscopic cross section for the ith type of process in cm^2. As mentioned previously, the microscopic cross section is usually expressed in units of barns.

As an illustration of how a particular type of cross section can be used to obtain spectral information, the following example is presented:

Let the activation cross section be a finite constant for all neutron energies greater than E_1 and less than E_2 and zero for all other energies. A graphical plot of this highly idealized cross section is given in Fig. 1.

Upon irradiation in an unknown flux, $\phi(E)$, the total flux between E_1 and E_2 can be determined as the integral of the differential flux. This is shown by the following:

$$\text{Reaction Rate} = R = N\int_0^{\infty} \sigma_i(E)\,\phi(E)\,dE = N\sigma_i\int_{E_1}^{E_2}\phi(E)\,dE$$

Solving for the total flux integral:

$$\int_{E_1}^{E_2}\phi(E)\,dE = \frac{R}{N\sigma_i}$$

It is assumed that the result of the ith type of transmutation gives an isotope whose quantity at any time can be determined, that the foil did not perturb the flux, and that the flux is time independent.

Threshold Type Foils

A graphical plot of the idealized threshold type cross section is shown in Fig. 2.

From the calculus, a result similar to the one previously obtained can be derived as shown below*:

$$A = \int_0^{\infty}\phi(E)\,\sigma_i(E)\,dE = \bar{\sigma}_i\int_{E_j}^{\infty}\phi(E)\,dE = \bar{\sigma}_i\bar{\phi}(E_j) \qquad (3)$$

It is seen that this type of foil will determine the total neutron flux above E_j. If several foils are used which have differing E_j's, it is possible to determine, in theory, the total flux between any two thresholds. In this manner, a histogram type of spectra representation

* $A = \frac{R}{N}$ and will be called the "saturated activity".

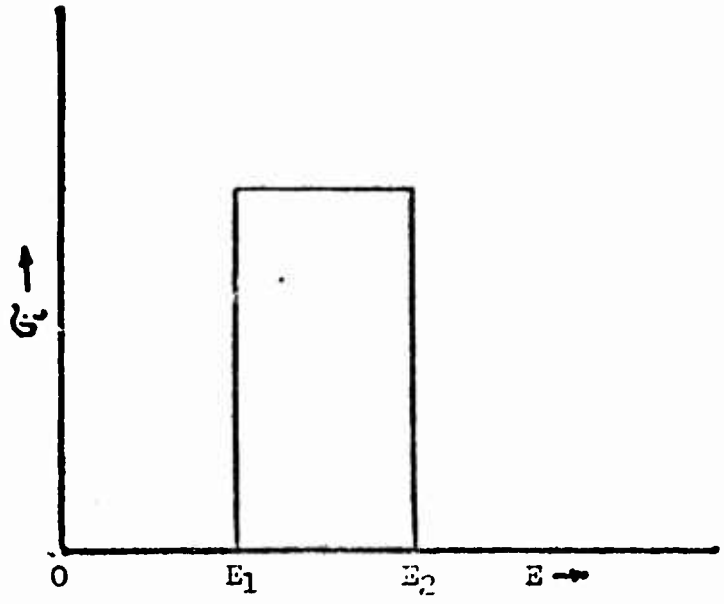

Figure 1

A Hypothetical Cross Section

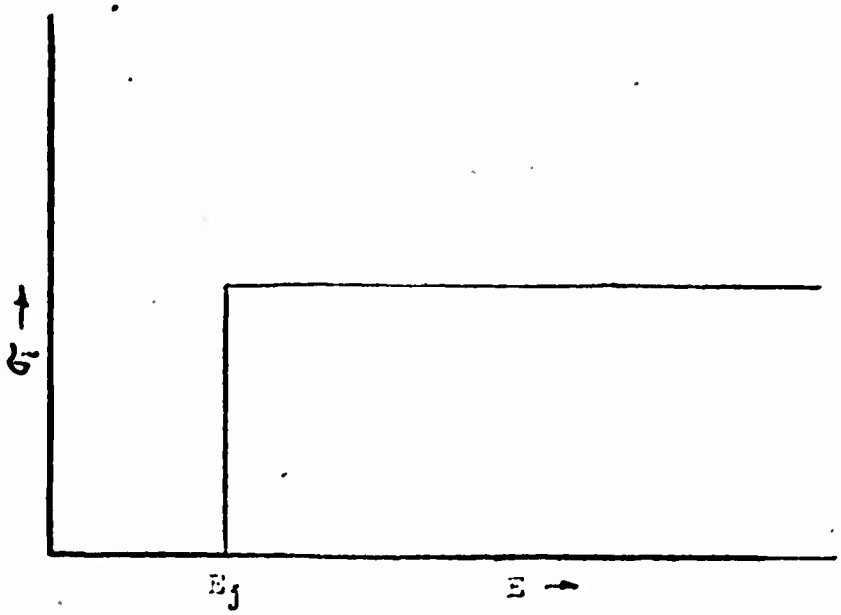

Figure 2

An Idealized Threshold-Type Cross Section

can be generated by simple subtraction.

Unfortunately, no materials exhibit such an idealized threshold. Figure 3 is a graphical presentation, with curve smoothing, of the cross sections of some of the commonly used threshold type foils. The fast fission foils are included for they also are of this nature, indeed even more so.

The variability and non-analytical behavior of these cross sections are responsible for the difficulty in obtaining good spectral information from foil measurements.

Resonance Type Foils

If the foil cross section shown in Fig. 1 were of such a width in energy that $\phi(E)$ could be considered a constant in this range, then by the calculus:

$$A = \int_0^{\infty} \phi(E)\ \sigma_i(E)dE = \bar{\sigma}_i\ \phi(E_1)\left[E_2 - E_1\right] \qquad (4)$$

Where $\phi(E_1) = \phi(E_2) =$ a constant.

By this method, the differential flux at E_1 can be obtained. If several foils with narrow and separated reaction intervals (E_1 to E_2) were available, the differential flux at the pertinent energies could be obtained. Drawing a smooth curve through the plotted points would yield a reasonable graph of the differential neutron flux (excluding fine structure). If materials existed with these cross section characteristics and if their reaction intervals were sufficiently separated so that the total energy interval would be 1 ev to 10 Mev, then the

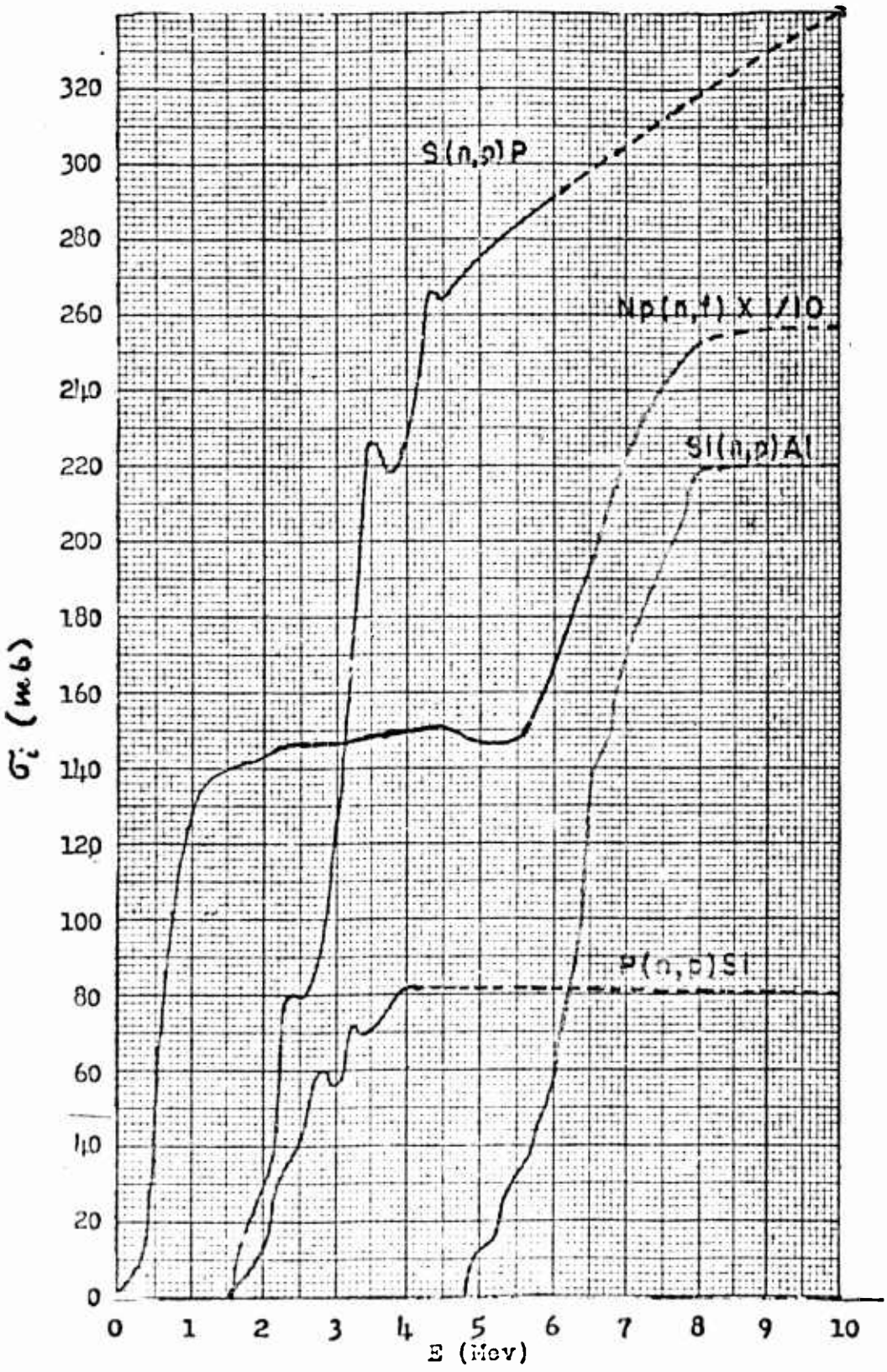

Figure 3

Cross Sections of Actual Threshold Type Foils

problem of obtaining a neutron flux-spectrum would be greatly reduced. Unfortunately, this is not the case.

The resonance type foils that have been used in the past have cross sections obeying, in general, the Briet-Wigner relationship. Few of these cross sections have actually been measured directly, but semi-quantitative values can be calculated by using the Briet-Wigner formula with the measured energy widths, peak energies, and/or maximum cross sections [4:15]. A simpler cross section parameter is the empirically determined resonance activation integral; however, reliance on resonance integrals often leads to misleading and inaccurate results because of the difficulty in taking into account all the necessary corrections.

For a more complete discussion on the resonance problem, the reader is invited to read Hughes' Pile Neutron Research. Suffice it to say here that a real cross section problem exists in the resonance region, that is, between 100 Kev and .025 ev.

III. The Trice Method and the Cadmium Difference Method

Introduction

Present evidence indicates that, in general, any reactor neutron spectrum above the thermal energies may be divided into two parts. One of these exists at energies greater than 1 Mev and has the general characteristics of a fission spectrum. The other, a result of neutrons being "slowed-down" by elastic collisions, occurs at energies below 1 Mev and has an approximate $1/E$ behavior. Although these general postulates are crude, they have been used with notable success.

For lack of a more appropriate name, the fast neutron technique discussed in this section is called the "Trice Method". Mr. J. B. Trice, then of the Oak Ridge National Laboratory, originally instructed the author in the usefulness of this method.

The method used for the $1/E$ spectral region is commonly called the "Cadmium Difference Method".

The Trice Method

Threshold and fast fission type foils are used to determine the flux-spectra in the fast neutron region (Mev region), for effective threshclds of presently available materials range from approximately 0.7 to 8 Mev.

The probability of finding a spectrum with the general characteristics of a fission spectrum indicates a method by which the actual fast-neutron cross sections can be transformed into idealized threshold types. This is done by using the activation formula, Eq. (2), to determine an effective threshold, E_e.

The calculational techniques are as follows:

1. A value of an effective cross section is selected; this is denoted as $\bar{\sigma}$, a constant. (The value of the cross sections near the effective threshold are the most important because of the decrease of flux with energy.)

2. The activation integral is equated to the simplified integral.

$$\int_0^{\infty} \sigma(E)\,\phi(E)\,dE = \bar{\sigma}\int_{E_e}^{\infty} \phi(E)\,dE$$

3. $\phi(E)$ is assumed to have the form of a fission spectrum*. The following representations have been proposed:

$\phi(E) \propto e^{-E} \sinh\sqrt{2E}$ (Watt)(5) [13: -] or,

$\phi(E) \propto e^{-E/.965} \sinh\sqrt{2.29E}$ (Univ. of "California") (6) [1: 662-670]

4. Using the tabulated $\phi(E)$ values, the activation integral is numerically integrated.

5. The value of the simplified integral is found.

$$\int_{E_e}^{\infty} \phi(E)\,dE = \frac{1}{\bar{\sigma}} \int_0^{\infty} \sigma(E)\ \phi(E)\,dE$$

* These functions, normalized to unit area, are tabulated in Appendix C.

6. E_e is determined from the $\phi(E)$ tabulation. In this manner, the true cross section is replaced by a step function, the threshold energy being determined by the expected spectral form, the fission spectrum.

As an example, a calculation is made of the P^{31} (n, p) Si^{31} effective threshold.

$$\int_0^{\infty} \sigma(E)\ \phi(E)dE = 23.65 \quad \text{(using California spectra)}$$

$$\bar{\sigma} = 80 \text{ mb}$$

$$\frac{23.65}{80} = \int_{E_e}^{\infty} \phi(E)dE = .296$$

from $\phi(E)$ tabulation, $E_e = 2.5$ Mev.

Figure 4 shows the transformation made in the P^{31} (n, p) Si^{31} cross section by this method.

A list of the effective thresholds and saturation cross sections for several materials are listed in Table 1.

In an actual experiment, the foils are not usually irradiated to saturation and are not counted immediately after irradiation. The following formula, derived in the standard manner, gives the approximate value of the integral flux from the experimentally determined activity:

$$\Phi(E_e) = \int_{E_e}^{\infty} \phi(E)\, dE = \frac{S}{N_0 \bar{\sigma}} \cdot \frac{e^{\lambda T}}{1 - e^{-\lambda t}} \cdot \frac{1}{\epsilon} \qquad (7)$$

Where: S = activity at T time after irradiation in dis/sec·mg.

$\bar{\sigma}$ = microscopic cross section in cm^2.

N_o = atoms/mg of pure isotope present.

λ = decay constant of transmutation product or $.693/T_{1/2}$

$\Phi(E_e) = \int_{E_e}^{\infty} \phi(E)\,dE$, the total neutron flux above the energy E_e---the integral flux.

$\phi(E)$ = differential neutron flux, see Eq. (2).

T = time after irradiation.

t = irradiation time.

ϵ = counter efficiency

By using several different foils, it is possible to make a plot of the integral flux versus energy. If the curve drawn through the experimentally determined points does not approximate a fission spectrum, the validity of the spectral knowledge gained is uncertain. Another defect is that the true cross sections are not most advantageously used when they are transformed to a step function.

An investigation has been made as to the degree to which this method will predict the correct spectrum in the absence of a fission spectrum. The numerical results of this test are shown in Fig. 5 and 6. The spectra assumed were as follows:

1. $\phi(E)$ = .0715 per Mev for E less than 14 Mev.
   $\phi(E)$ = 0 for E greater than 14 Mev. (8)
2. $\phi(E)$ = .38 per Mev for E greater than 0 Mev and less than 1 Mev.

Table I

Table of (n,p), (n,α), and (n, f) Threshold Reactions

Reaction	E_e (Mev)	$\bar{\sigma}$ (barns)	Half Life of Product
P^{31} (np) Si^{31}	2.5	.075(a)	2.62 h
S^{32} (np) P^{32}	2.9	.300(b)	14.3 d
Al^{27} (np) Mo_0^{27}	5.3	.080(a)	9.8 m
Ni^{58} (np) Co^{58}	5.0	1.23 (c)	72 d
Si^{28} (np) Al^{28}	6.1	.190(d)	2.3 m
Mg_0^{24} (np) Na^{24}	6.3	.048(c)	15.0 h
Al^{27} (nα) Na^{24}	8.6	.110(e)	15.0 h
Np^{237} (nf)	.75	1.52 (a)	See Text
U^{238} (nf)	1.45	.54 (a)	
Th^{232} (nf)	1.75	.15 (a)	

(a) Ref. 3, page 105.

(b) Ref. 3, page 108, and Ref. 7, page 106.

(c) Ref. 2, page 29.

(d) Ref. 9, page 248. BNL-325 value at 14 Mev used for normalization.

(e) Ref. 12, page 343. BNL-325 value used for normalization.

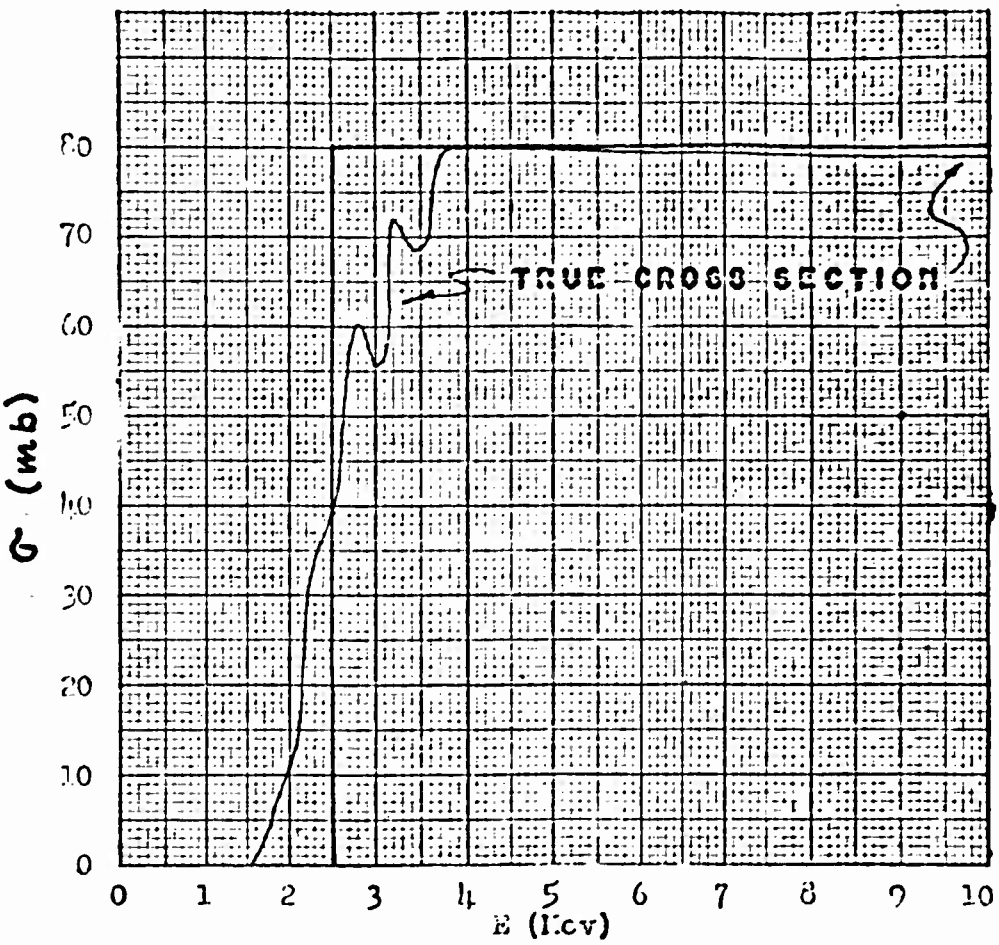

Figure 4

Trico Transformation

of

$P^{31}(n,p)Si^{31}$ Cross Section

ϕ (E) = .38/E per Mev for E greater than 1 Mev and less than 14 Mev.

ϕ (E) = 0 for E greater than 14 Mev. (9)

3. ϕ (E) = .0102(14-E) per Mev for E less than 14 Mev.

ϕ (E) = 0 for E greater than 14 Mev. (10)

4. ϕ (E) = $.454e^{-E/.965} \sinh\sqrt{2.29E}$ per Mev for all E (California fission spectrum).

In view of the errors encountered in making any foil measurement, it is apparent that the Trice Methods give reasonable results ($\pm$ 50%) even when the actual spectrum differs vastly from the fission spectrum. By making a correct assumption regarding the true spectrum, it is, of course, possible to calculate the thresholds in such a manner as to get correct results; however, the labor involved in doing this would not be insignificant.

In a thermal reactor, a spectrum having a shape combining a fission and a $\frac{1}{E}$ spectrum is anticipated. For this type of situation, it appears that the Trice Method would give quite acceptable results.

As an illustration of an actual reactor measurement, Fig. 7 is a plot of a portion of the results obtained at the Materials Testing Reactor in 1954. The prediction of this data is that the spectrum measured is very close to a pure fission spectrum.

The fission rate (equivalent to saturated activity) of fast-fission foils can be found by extrapolating from the fission product decay curve [6:153-156], or by using a fast-neutron fission chamber.

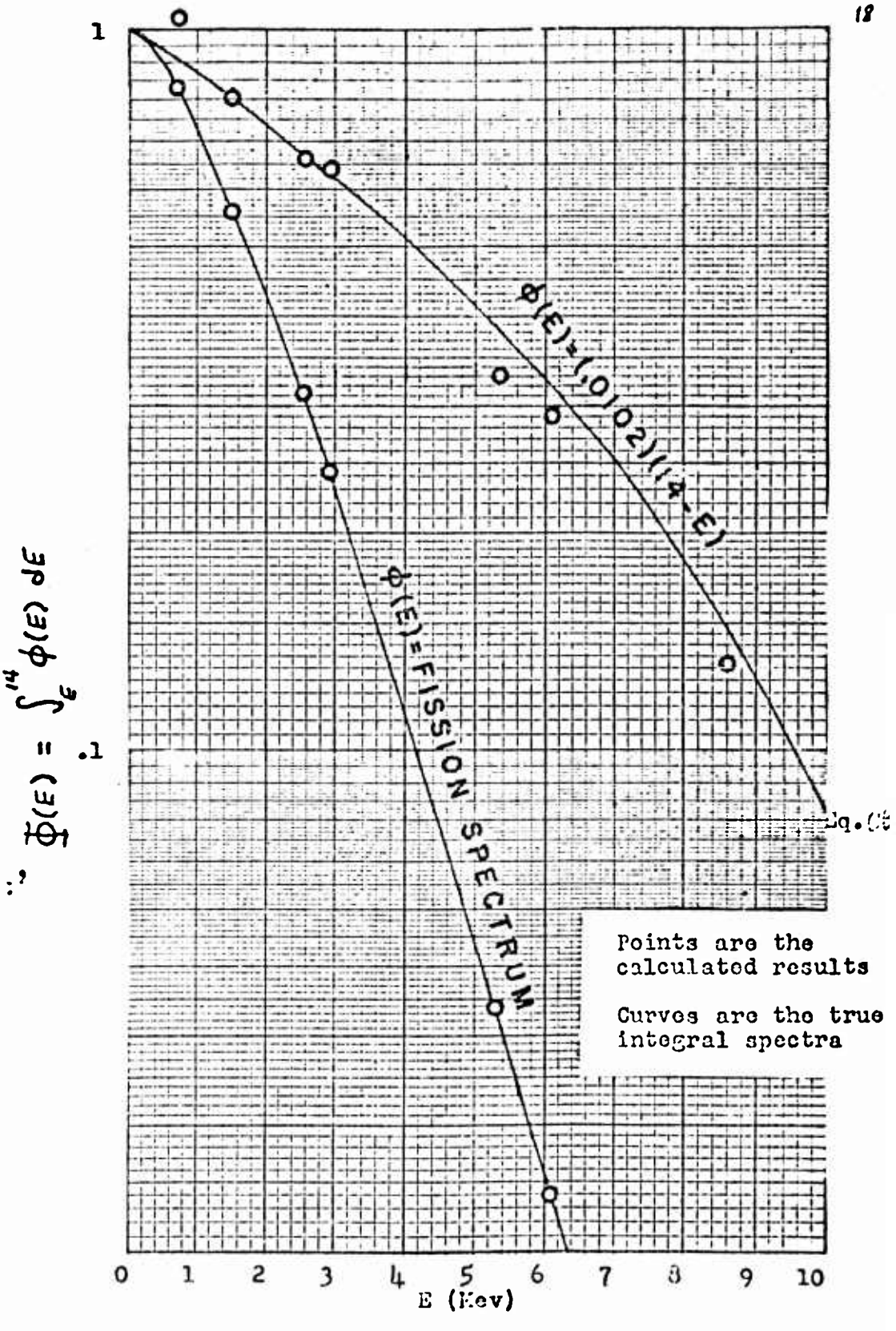

Figure 5

Prediction of Spectra by the Trico Method

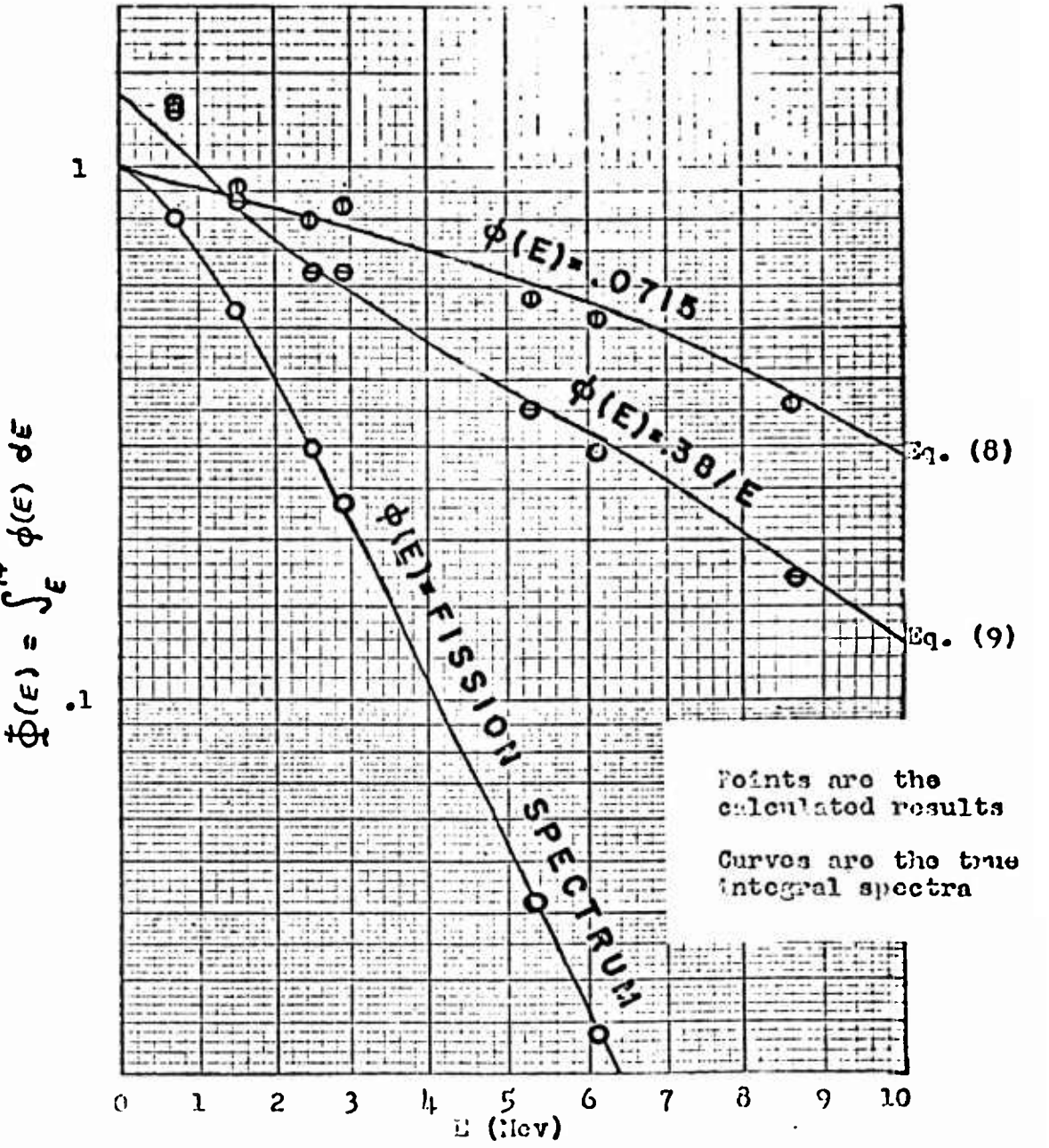

Figure 6

Prediction of Spectra by the Trice Method

In neutron fluxes above 10^{9} neuts/cm^2·sec, only the first technique is presently suitable [10:16]. G. S. Hurst has found that the fission product gamma decay rate (greater than 1 Mev) is essentially the same for plutonium-239, neptunium-237, and uranium-238, and is apparently independent of neutron energy. The details of this analysis are not presented here, but can be found in Ref. 5 and 6.

The Cadmium Difference Method

The Cadmium Difference Method utilizes the resonance activation integral of resonance type foils to achieve spectral knowledge in the 1/E region. The predominate reason for this is that the resonance integral is better known than the true cross section. The discussion is restricted to materials having resonances at energies greater than 100 ev. The resonance absorption by cadmium and the shape of the cadmium transmission curve are not important above this energy.

$$\text{Resonance integral} = \int_{.4\ ev}^{\infty} \sigma \, dE/E. \qquad (11)$$

It is assumed that .010 inch cadmium covers are used, an isotropic flux distribution exists, and the material is present in such small quantities so as not to perturb the flux in the resonance region.

For a pure 1/v activation in a dE/E type of flux, the thermal cross section (2200 m/sec) is two times the activation integral. This is shown by the following:

$$\sigma = \frac{1}{v} \text{cross section} = \frac{k}{\sqrt{E}} \text{ where K is a constant.}$$

GNE-9

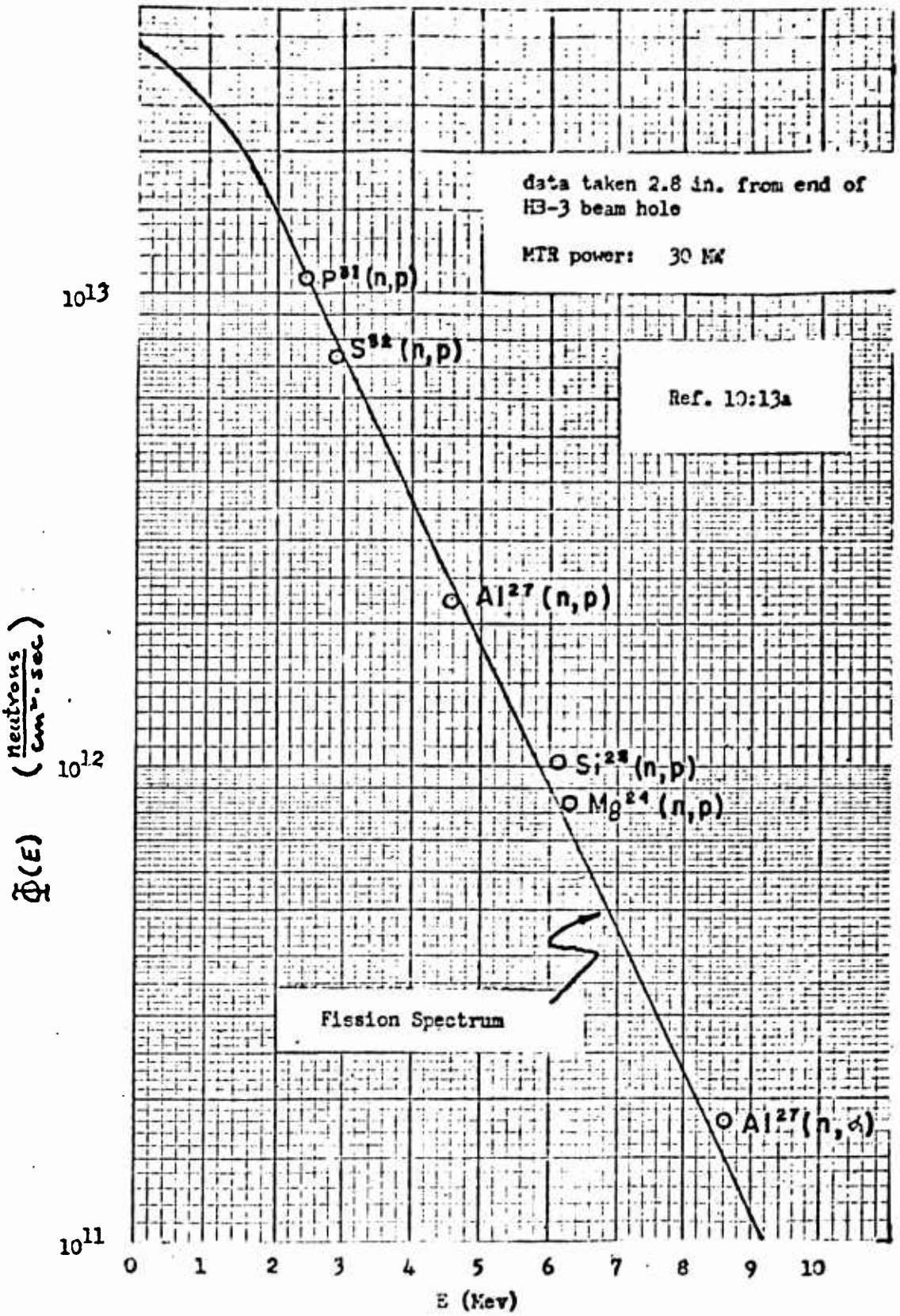

Figure 7

Fast-Neutron Flux Above Threshold vs. Threshold

$$\frac{\sigma_{th}}{\int_{.4}^{\infty} \sigma \, dE/E} = \frac{k/\sqrt{E_n}}{\int_{.4}^{\infty} k \, dE/E^{3/2}} = \frac{1/\sqrt{.025}}{2/\sqrt{.4}} = 2.0 \qquad (12)$$

The total epi-cadmium activation is proportional to

$$\int \sigma_{1/v} dE/E + \int \sigma_{res} dE/E = (1+\Delta) \int \sigma_{1/v} dE/E = \frac{(1+\Delta)}{2} \sigma_{th} \qquad (13)$$

$$\Delta = \frac{\int \sigma_{res} \, dE/E}{\int \sigma_{1/v} \, dE/E} = \frac{\text{resonance activation}}{1/v \text{ activation}} \qquad (14)$$

When the foil is irradiated without cadmium (bare), the total activation is given by the following:

$$A_{bare} = \phi_{th} \sigma_{th} + \zeta_0 \int_{E^1}^{\infty} \frac{\sigma \, dE}{E} \qquad (15)$$

Where: A_{bare} = the saturated activity without cadmium.

ϕ_{th} = the thermal neutron flux --- the total thermal neutron density times 2.2×10^5 cm/sec.

σ_{th} = the 2200 m/sec activation cross section.

ζ_0 = $E\phi(E)$, a constant.

σ = the activation cross section as a function of energy.

E^1 = the energy at which the resonance flux joins the thermal flux.

The lower limit of the above integral is taken as E^1, for in an actual activation some neutrons are absorbed in slowing down from .4 ev to thermal. The energy, E^1, for which the dE/E and the Maxwell distributions are equal in a graphite moderated, room temperature reactor is approximately .24 ev. The following calculation indicates the importance of this region for a pure 1/v foil.

$$\int_{.24}^{.4} \sigma \, dE/E = \sigma_{th} \int_{.24}^{.4} \frac{\sqrt{.025}}{E^{3/2}} dE = .12 \, \sigma_{th} \qquad (16)$$

The total activation of the foil irradiated with a .010 inch cadmium cover in an isotropic 1/E flux is as follows:

$$A_{cd} = \phi_o \int_{.4}^{\infty} \sigma \frac{dE}{E} \qquad (17)$$

Irradiated without cadmium, the total activation is as follows:

$$A_B = \phi_{th} \sigma_{th} + \phi_o \int_{.24}^{.4} \sigma \frac{dE}{E} + \phi_o \int_{.4}^{\infty} \sigma \frac{dE}{E}$$

$$= \phi_{th} \sigma_{th} + \phi_o (.12 \sigma_{th}) + \phi_o \int_{.4}^{\infty} \sigma \, dE/E \qquad (18)$$

The cadmium ratio, CR, is given by the following:

$$CR = A_B / A_{Cd} = 1 + \frac{\phi_{th}\,\sigma_{th} + .12\,\phi_0\,\sigma_{th}}{\phi_0 \int_{.4}^{\infty} \sigma\, dE/E} \qquad (19)$$

$$CR - 1 = \frac{\sigma_{th}\,(\phi_{th} + .12\,\phi_0)}{\phi_0 \int_{.4}^{\infty} \sigma\, dE/E} \qquad (20)$$

Now, ϕ_0 is usually much less than ϕ_{th} ($\phi_{th}/\phi_0 \simeq 100$); therefore, the $.12\,\phi_0 \simeq .001\,\phi_{th}$ and can be neglected.

$$CR - 1 = \frac{\sigma_{th}\,\phi_{th}}{\phi_0 \int_{.4}^{\infty} \sigma\, dE/E} \qquad (21)$$

Rearranging,

$$\phi_0 = \frac{\sigma_{th}\,\phi_{th}}{(CR-1) \int_{.4}^{\infty} \sigma\, dE/E} \qquad (22)$$

But,

$$\int_{.4}^{\infty} \sigma\, dE/E = (1+\alpha) \int_{.4}^{\infty} \sigma_{1/v}\, dE/E = \frac{(1+\alpha)}{2}\,\sigma_{th}$$

So,

$$\phi_o = \frac{2\phi_{th}}{(CR-1)(1+\varepsilon)} \qquad (23)$$

The usual practice in making a measurement in the 1/E region is to determine the thermal flux by cobalt, gold, or indium irradiation. The cadmium ratio of several of the detectors listed in Table 2 is then determined by irradiation and counting. If the spectrum is indeed the 1/E type, the ϕ_o determined for each resonance detector should be the same. The differential flux is then given to be the following:

$$\phi(E) = \phi_o / E \qquad \text{(over the range of energy determined by the detectors.)} \qquad (24)$$

If the ϕ_o's are not approximately the same, little can be said about the spectrum.

In all such measurements, care should be taken to insure that the correct cadmium thicknesses are used (in the above example .010 inches), and that the resonance detectors used do not appreciably perturb the flux. In addition, it is not usually advisable to irradiate bare and cadmium covered foils in the same location at the same time.

Discussion and Conclusions

By combining the results obtained by threshold and resonance type foils, a crude picture of the neutron flux-spectrum of a reactor can many times be obtained. A 1/E extrapolation from 9100 ev to the point

at which it meets the threshold foil curve is usually made; however, this does not imply measured results in this region. At the low energy end of the spectrum, the spectrum is assumed to be 1/E down to E^1.

Table 2

Table of Resonance Parameters

Reaction $X(n,\gamma)X^{+1}$	Resonance Energy (ev)	α_1	α_2	Half Life of Product
Cobalt-59	120	2.0	—	5.3 y
Manganese-55	260	1.0	1.33	2.6 h
Copper-63	570	1.3	.933	12.8 h
Sodium-23	1710	~ 0	.238	15. h
Chlorine-37	1800	~ 0	.079	38. m
Vanadium-50	3000	~0	.134	3.74 m
Aluminum-27	9100	.68	.159	2.3 m

α_1's calculated from data presented in Reference 8.

α_2's obtained from Reference 10.

$$\phi_o = \frac{2.27\,\phi_{th}}{(CR-1)(1+\alpha_1)}$$ Using ~.020 in. cadmium (.5 ev cutoff)

$$\phi_o = \frac{1.43\,\phi_{th}}{(CR-1)(1+\alpha_2)}$$ Experimentally determined using .010" cadmium.

The α_1's listed above should not be used until checked in known 1/E spectrum.

IV. The Role of Orthogonality

Introduction

In the following sections, several flux-spectra analysis methods are discussed which require a minimum of spectral assumptions and which use the activation cross sections of foils in their true form. That is, no approximations regarding step functions are made. Before progressing with a discussion of these methods in detail, it is best to discuss them in a general manner.

The general procedure has been to express the activations as a linear combination of terms which depend upon some parameter describing the spectrum. The number of the equations is equal to the number of foils used.

A general requirement in the solution of systems of equations is that the equations themselves be independent. Since any analytical method of obtaining flux-spectra information from foils will be dependent upon the foil cross sections, it is obvious that these functions must not be too similar.

Two functions are said to be orthogonal if

$$\int_0^{\infty} X_i(E)\, X_j(E)\, dE \simeq C \qquad (25)$$

Where, $X_i(E)$ and $X_j(E)$ are the functions.

As a definition, $X_i(E)$ is said to be "independent" of $X_j(E)$ if the above integral is true.

If $\int_0^{\infty} X_i^1(E)X_j^1(E)dE = 0$, $X_i^1(E)$ and $X_j^1(E)$ are said to be "dependent". The functions X^1 have been normalized so that:

$$\int_0^{\infty} \left[X^1(E)\right]^2 dE = 1$$

When the value of the orthogonality integral is between 0 and 1, the functions are said to be partially "dependent", the degree of "dependency" hinging on the magnitude. (The orthogonality integral, as used here, is really the inner product of two normalized vector functions in Hilbert space --- the magnitude being the cosine of the apparent angle between the functions.)

Threshold Type Foils

In practical cases, the cross sections of the threshold and fast fission materials are not orthogonal. That is,

$$\int_0^{\infty} \sigma_i(E)\, \sigma_j(E)dE \neq 0 \qquad (2.6)$$

As a simple illustrative example of what can occur in solving nearly dependent equations, the following is presented:

Let two hypothetical parameters, X and Y, be represented by the following equations:

$$10X + 2Y = 24 = A$$

$$9X + 2Y = 20 = B$$

The solution is: $X = 4$

$Y = 8$

Now, let there be a four per cent error in A. Then,

$10X + 2Y = 23$

$9X + 2Y = 20$

The solution is: $X = 3$

$Y = -3.5$

This result shows that an error of less than 5% in A will change the calculated value of Y by more than 50%.

Let it be assumed for a moment that X and Y are spectral parameters, and A and B are foil activations. Then the coefficients of X and Y must be related to the activation cross sections, for the cross sections are the connecting "links" between flux and activation. Now an experimental activation error of 5% is certainly not unreasonable; however, this error would generate an error of over 50% in one of the calculated spectral parameters. The reason for this is that the coefficients are nearly proportional; the system of equations is said to be "poorly conditioned".

The preceding discussion implies that difficulty may be experienced in accurately determining spectral parameters from any system of equations in which two or more cross sections are quite "dependent".

As a useful technique in reducing this problem, use is made of the following identity*:

* See Appendix D for derivation.

$$A = \int_0^{\infty} \phi(E)\,\sigma(E)\,dE = \int_0^{\infty} \Phi(E)\,\frac{d\sigma}{dE}\,dE \qquad (27)$$

Where, $\Phi(E) = \int_E^{\infty} \phi(E')\,dE'$ (the integral flux).

Since threshold detector cross sections increase rapidly near their thresholds, $\frac{d\sigma}{dE}$ is largest in the threshold region and quite small elsewhere (see Fig. 3). Using the alternative activation representation, it may be possible to solve a system of equations for Φ with less error even though the cross sections are "dependent", for the derivatives of the cross sections may be quite "independent".

Since threshold type foils are used in the fission spectrum region, and the flux (either integral or differential) decreases rapidly in this region, it is convenient to introduce the following relationships:

$$\Phi = \Phi_{F.S.}\,\Phi' \qquad (28)$$

Where, $\Phi_{F.S.}$ = the integral fission spectrum function.

Φ' = the ratio of the true integral spectrum to the integral fission spectrum. This term is fairly constant in energy.

Φ = the true integral spectrum.

Now, the activation equation can be written as the following:

$$A = \int_0^{\infty} \Phi'\,\Phi_{F.S.}\,\frac{d\sigma}{dE}\,dE \qquad (29)$$

Since Φ' is fairly constant in energy, a set of threshold type foils can be considered as "independent" if :

$$\int_0^\infty \Phi'^2_{F.S.} \frac{d\sigma_i}{dE} \frac{d\sigma_j}{dE} dE = 0 \qquad (30)$$

for all $i \neq j$ detectors.

The above equation defines orthogonality of the cross section derivatives with respect to the parameter $\Phi'^2_{F.S.}$.

Resonance Type Foils

As previously discussed, the cross sections of resonance type foils are characterized by resonance peaks superimposed on a 1/v distribution. Since the resonance peaks of the detectors are generally narrow and separated in energy, it might be supposed that the cross sections are orthogonal. Unfortunately, this is true only if the 1/v portion can be eliminated from the overall activation. If the α's, Eq. (14), of several foils are much greater than unity, the 1/v activation can be neglected; if the α's are less than unity, the major contribution to the activation is due to the 1/v cross section. Since most presently used foils have significant 1/v cross sections and small α's, they are highly "dependent". Since the integrals of the alternating cross sectional derivatives are nearly zero, they are not suitable for making integral spectrum measurements; however, they are suited for making integral spectrum measurements if α is large. One practical solution to this α problem is discussed in Appendix E.

Since at this writing, there is a lack of good resonance cross section data, the usefulness of any analytical method utilizing true cross sections is somewhat academic. If and when such cross sections become available, the resonance type foil may become a very useful device for measuring the differential spectrum in the epithermal energy region.

V. The Polygonal Method

Basic Philosophy

The basic postulate of this method is that true spectrum parameters can be represented by a linear interpolation between a fixed number of empirically determined spectrum values. Figure 8 is a graphical representation in energy space of this postulate. In this case the ϕ_i's are taken as the quantities to be determined by activation and calculation.

Since the true spectrum is probably a smooth curve, a certain amount of error should be expected from such a representation in energy space. By transforming the energy variable into a more appropriate variable, it should be possible to greatly reduce this error. Some possible transformations are discussed later in this section.

With five unknown ϕ's, as indicated in Fig. 8, five different foils with independent cross sections would be required for their determination (five unknowns --- five independent equations).

Application to Threshold Type Foils

General Equations in Energy Space. As discussed previously, threshold type foils are most suited for integral spectral measurements in the Mev region (plutonium-239 is an exception to this rule). The following equations describe the polygonal method in the simplest mathematical sense; that is, all correction factors, counter geometries,

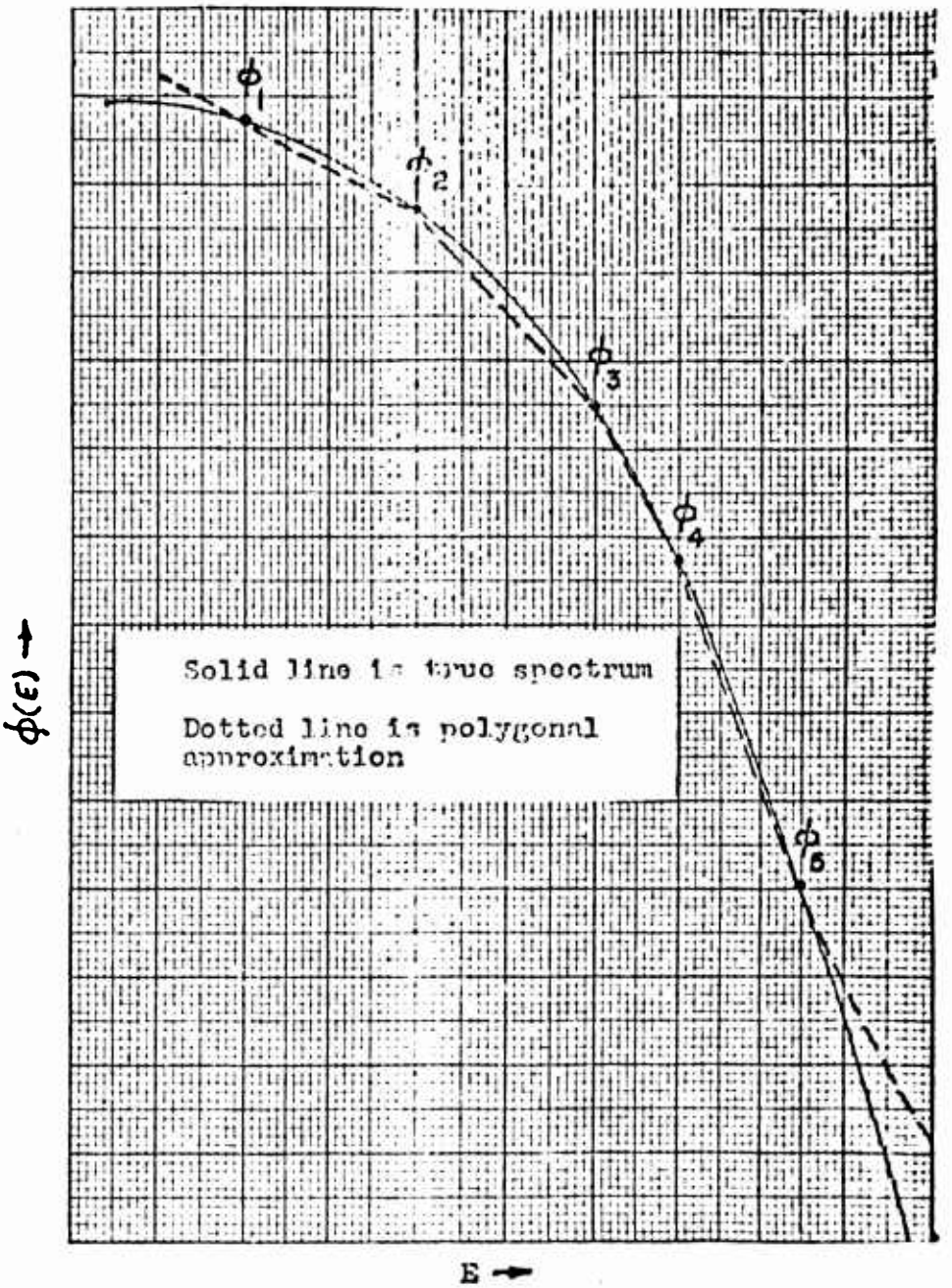

Figure 8

Graphical Representation

of

Polygonal Method

nuclear densities, etc., are assumed to be included in the saturated activity terms (A_i). For reasons of convergence and convenience, the spectrum is assumed to be exponentially decreasing above E_N. The energy value E_N corresponds to the highest energy spectral parameter (the energy corresponding to the ϕ_5 value in Fig. 8).

The General Activation Equation is as follows:

$$A_i = \int_0^{E_1} \frac{E}{E_1} \phi_1 \sigma_i(E)\, dE + \int_{E_1}^{E_2} \left[\phi_1 + \frac{E-E_1}{E_2-E_1}(\phi_2-\phi_1)\right] \sigma_i(E)\, dE$$

$$+ \int_{E_2}^{E_j} \left[\phi_2 + \frac{E-E_2}{E_j-E_2}(\phi_j-\phi_2)\right] \sigma_i(E)\, dE + \cdots \int_{E_N}^{\infty} \phi_N e^{-\gamma_2(E-E_N)} \sigma_i(E)\, dE \qquad (31)$$

Where: A_i = saturated activity of i_{th} foil.

ϕ_1 = differential flux at energy E_1.

ϕ_j = differential flux at energy E_j.

σ_i = activation cross section of ith foil.

ϕ_N = differential flux at energy E_n.

N = number of different foils used.

For N foils, there will exist N equations of the above type. By algebraic manipulation, these equations are transformed into the following:

$$A_1 = C_{11}\phi_1 + C_{12}\phi_2 + C_{13}\phi_3 + \cdots C_{1N}\phi_N$$
$$\vdots$$
$$A_i = C_{i1}\phi_1 + C_{i2}\phi_2 + C_{i3}\phi_3 + \cdots C_{iN}\phi_N$$
$$\vdots$$
$$A_N = C_{N1}\phi_1 + C_{N2}\phi_2 + C_{N3}\phi_3 + \cdots C_{NN}\phi_N \qquad (32)$$

Where:

$$C_{i1} = E_1 \int_0^{E_1} \sigma_i(E)\, dE/E + \left(1 + \frac{E_1}{E_2 - E_1}\right) \int_{E_1}^{E_2} \sigma_i(E)\, dE - \frac{1}{E_2 - E_1} \int_{E_1}^{E_2} E\, \sigma_i(E)\, dE$$

$$C_{ij} = \left(1 + \frac{E_j}{E_{j+1} - E_j}\right) \int_{E_j}^{E_{j+1}} \sigma_i(E)\, dE - \frac{E_{j-1}}{E_j - E_{j-1}} \int_{E_{j-1}}^{E_j} \sigma_i(E)\, dE$$

$$+ \frac{1}{E_j - E_{j-1}} \int_{E_{j-1}}^{E_j} E\, \sigma_i(E)\, dE - \frac{1}{E_{j+1} - E_j} \int_{E_j}^{E_{j+1}} E\, \sigma_i(E)\, dE$$

For $j = 2, 3, 4, \cdots N-1$

$$C_{iN} = \int_{E_N}^{\infty} e^{-.72(E - E_N)} \sigma_i(E)\, dE + \frac{1}{E_N - E_{N-1}} \int_{E_{N-1}}^{E_N} E\, \sigma_i(E)\, dE - \frac{E_{N-1}}{E_N - E_{N-1}} \int_{E_{N-1}}^{E_N} \sigma_i(E)\, dE$$

(33)

In matrix symbolism:

$$(A) = (C)\ (\phi) \tag{34}$$

Solving for ϕ :

$$(\phi) = (C)^{-1}\ (A) \tag{35}$$

Since threshold detectors are most suitable for determining integral flux, $\underline{\Phi}(E)$, the inverse (C) matrix should be multiplied by the integral matrix, (I).

$$(\underline{\Phi}) = (I)\ (\phi) = (I)\ (C)^{-1}\ (A) \tag{36}$$

For this particular polygonal method, the (I) matrix is the following:

$$(I) = \begin{pmatrix} \Delta_1 E_2/2 & \frac{\Delta_1 E_2 + \Delta_2 E_3}{2} & \cdots & \frac{\Delta_{N-1} E_N}{2} + 1.39 \\ — & \Delta_2 E_2/2 & \cdots & \frac{\Delta_{N-1} E_N}{2} + 1.39 \\ \vdots & \vdots & \vdots & \vdots \\ — & — & — & 1.39 \end{pmatrix} \tag{37}$$

Note that all elements to the left of the diagonal are zero.

The construction of the integration matrix is based upon the following:

$$\Phi_1 = \int_{E_1}^{\infty} \phi(E)\,dE = \left[\frac{\phi_1 + \phi_2}{2}\right] \Delta_1 E_2 + \left[\frac{\phi_2 + \phi_3}{2}\right] \Delta_2 E_3$$

$$+ \left[\frac{\phi_3 + \phi_4}{2}\right] \Delta_3 E_4 + \cdots \left[\frac{\phi_{j-1} + \phi_j}{2}\right] \Delta_{j-1} E_j +$$

$$\cdots 1.39\,\phi_N \qquad (38)$$

Where: $\Delta_{j-1} E_j = E_j - E_{j-1}$

The last term is $1.39\phi_N$, for $\int_{E_N}^{\infty} e^{-.72(E-E_N)}\,dE = 1.39$

In summary, the following procedure is indicated for obtaining integral spectrum information by this method:

1. Several foil materials whose cross sectional derivatives are quite independent are selected.

2. (C) is computed by "hand". A set of E_j's are selected for the integral limits; each is selected from the energy region in which the ith cross section is varying between its minimum and saturated value. (The E_j's selected by using the polynomial method described in the next section may be the best.)

3. $(C)^{-1}$ is computed by an electronic computer.

4. The (I) $(C)^{-1}$ matrix is computed for the E_j's used in the (C) calculation. An electronic computer is most conveniently used for this.

5. Upon completion of the nuclear measurement, (I) $(C)^{-1}$ is multiplied by the empirically determined A_i's (a simple "hand" calculation).

6. The result of step 5 yields the Φ_j's.

7. If the (I) $(C)^{-1}$ matrix is poorly conditioned, a new set of E_j's are selected and the calculation is repeated.

The Definition of Gay, Happy, and Sad. As mentioned previously, a spectrum having a form similar to the fission spectrum is expected to be found in the Mev region. This fission spectrum function is a rapidly decreasing function in energy; hence, the integral flux above 8 Mev is much less than that above 2. Since the polygonal method, in energy space, is based on a linear extrapolation between energy values, the error involved in approximating the true spectrum may be significant. The error involved is the integration error which results from approximating a continuously varying spectrum by chords (see Fig. 8). It is believed that better results may be obtained if a new function is generated that will give a linear formulation with regard to the fission spectrum, for the fission spectrum is a first approximation to a reactor generated fast neutron spectrum. If correctly determined, this new function would serve the same purpose in the Mev region as does lethargy in the 1/E region. Like lethargy flux in the 1/E region, the differential flux with respect to the new function would be a

constant in the Mev region. (The differential flux in energy would be sharply decreasing with increasing energy.)

It has been shown that the following is a fair approximation of the uranium-235 fission spectrum:

$$\phi(E) = C\sqrt{E}\ e^{-.775E} \qquad (39)[1:662]$$

where C is a constant.

The new function, called "gay", is defined so that:

$\phi(g)$ = a constant for a pure fission spectrum, where g = gay.

The derivation of gay is as follows:

$$\phi(E)\,dE = C\sqrt{E}\ e^{-.775E}\,dE = \phi(g)\,dg$$

$$\phi(g) = C\sqrt{E}\ e^{-.775E}\ dE/dg = \text{constant} = C_1$$

$$dg = C_1\sqrt{E}\ e^{-.775E}\,dE \qquad g = C_2\int_0^{E_0}\sqrt{E}\ e^{-.775E}\,dE$$

$$\text{let } \gamma = .775E \qquad d\gamma = .775\,dE$$

$$g = \frac{C_2}{.775}\int_0^{.775E_0}\sqrt{\frac{\gamma}{.775}}\ e^{-\gamma}\,d\gamma$$

$$g = C_3 \int_0^{.775 E_o} \sqrt{\gamma}\, e^{-\gamma} d\gamma$$

let $u^2 = \gamma \qquad 2u\,du = d\gamma$

So:

$$g = C_3 \int_0^{\sqrt{.775 E_o}} 2u^2 e^{-u^2} du$$

By parts:

$$g = C_3 \left[-u e^{-u^2} \Big|_0^{\sqrt{.775 E_o}} + \int_0^{\sqrt{.775 E_o}} e^{-u^2} du \right] \qquad (40)$$

The first term of the above equation can be evaluated directly; the integral can be evaluated by using tables of the standard error integral.

The constant, C_3, is arranged so that g_{max} is 1.0 --- this corresponds to an infinite energy. By numerical evaluation, C_3 has been calculated to be equal to 1.13. Figure 9 is a plot of gay versus energy.

The relationship between $\phi(g)$ and $\phi(E)$ is, by definition, the following:

$$\phi(E) = \phi(g) \frac{dg}{dE} = \phi(g)\, C\sqrt{E}\; e^{-.775E}$$

$$= \phi(g) \cdot \text{Fission Spectrum} \qquad (41)$$

Now, at any gay, the differential flux can be found by multiplying $\phi_c(E)$ in the fission spectra tabulation (Appendix C) by the appropriate value of $\phi(g)$.

For reasons of presentation clarity, $\phi(g)$ is called the "sad" flux; $\int_g^1 \phi(g)\,dg$ is called the "happy" flux. A reason for these names is that the integral of a poorly "behaved" function is better "behaved"; hence, "happy" is better "behaved" than is "sad".

General Equations in Gay Space. With the exception of the last term, the polygonal equations in gay space are identical in form to those in energy space. The A_i's, which must have the same numerical value as before, are as follows:

$$A_i = \int_0^{g_1} \frac{g_1}{g}\,\phi_1\,\sigma_i(g)\,dg + \int_{g_1}^{g_2} \left[\phi_1 + \frac{g-g_1}{g_2-g_1}(\phi_2-\phi_1)\right]\sigma_i(g)\,dg$$

$$+ \cdots \phi_N \int_{g_N}^{1} \sigma_i(g)\,dg \qquad (42)$$

Note that the Nth term is of different form.

Except for the C_{iN} coefficients, the general coefficients are identical in form to those used in energy space.

The Nth coefficient is as follows:

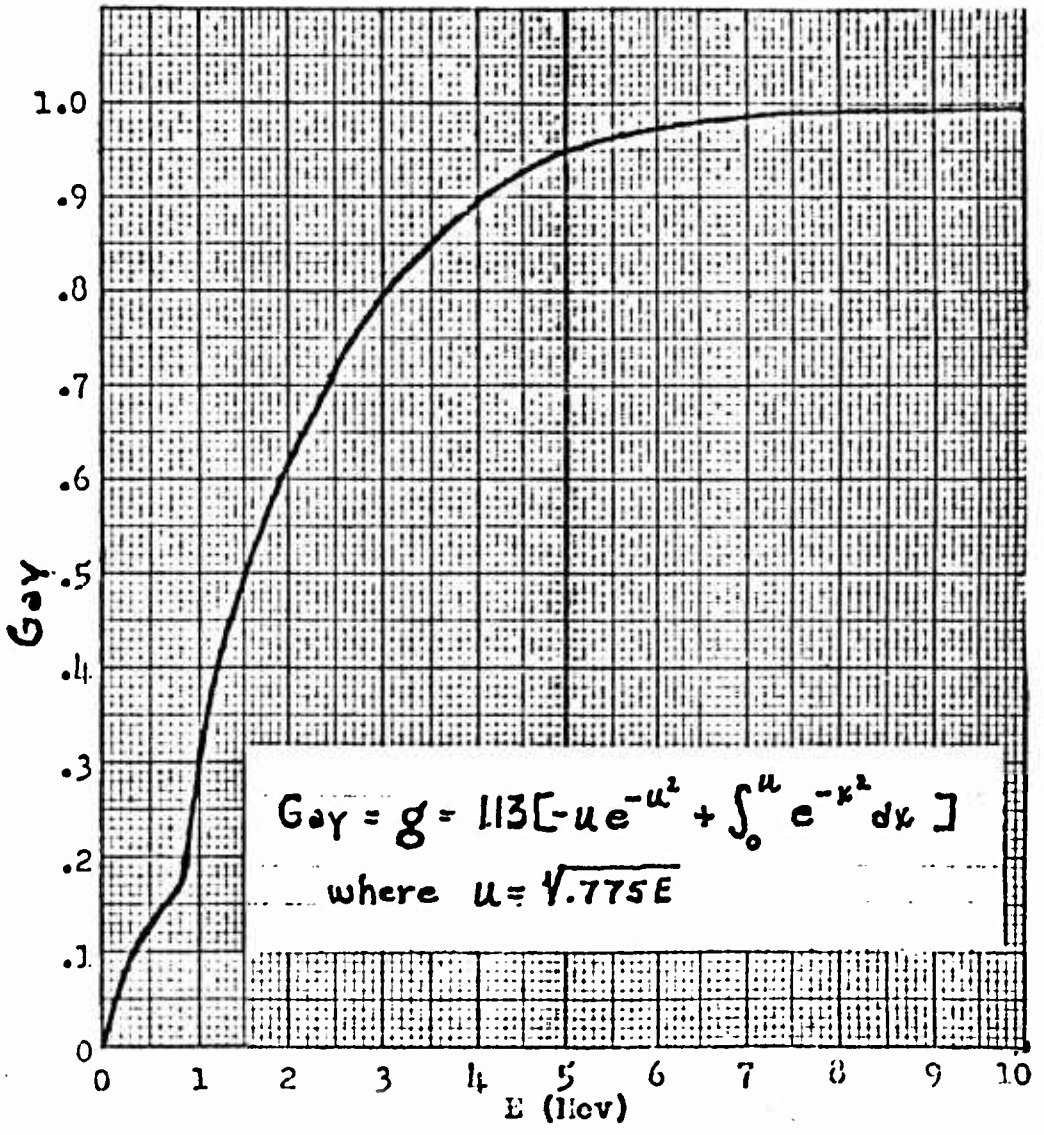

Figure 9

Plot of Gay vs. Energy

$$C_{iN} = \frac{1}{g_N - g_{N-1}} \int_{g_{N-1}}^{g_N} g\, \sigma_i(g)\, dg - \frac{g_{N-1}}{g_N - g_{N-1}} \int_{g_{N-1}}^{g_N} \sigma_i(g)\, dg$$

$$+ \int_{g_N}^{'} \sigma_i(g)\, dg \qquad (43)$$

The general procedure for utilizing this method is the same as that used in energy space. Once the happy flux is computed, the energy flux can be found by multiplying happy by the appropriate value in the fission spectrum tabulation.

Discussion and Conclusions. The determination of the proper E_j's or g_j's is probably the greatest problem encountered in using the polygonal method. Calculations using hypothetical cross sections have been made in the attempt to find some general selection criterion which would not involve numerical iteration procedures. The results of these calculations have not been successful; however, the energy parameters (E_j's) found to be suitable for the method described in the next section (the Polynomial Method) may be the correct ones to use. It is hoped that this can be investigated in the near future.

If cross sections existed which were of the idealized threshold type, then the proper E_j's or g_i's would be at the respective thresholds. On the other hand, in this pleasant situation the Trice Method would give equally accurate results.

Application to Resonance Type Foils

Whereas gay was believed to have general usefulness in the fission spectra region, it is believed that the best general function to be used in 1/E region is lethargy, u .

$$u = \ln \frac{E_0}{E} \qquad (44)$$

where E_0 is some arbitrarily selected high energy.

In a pure 1/E flux, $\phi(u)$ is a constant and is related to $\phi(E)$ by the following:

$$\phi(u) = E\phi(E) \qquad (45)$$

The general equations and coefficients of the polygonal method as applied to the 1/E region are of the same form as those used in the fission spectrum region. When used in the 1/E region, lethargy replaces gay, and the top limit of the last integral becomes zero if the calculation is taken to the E_0 of lethargy. It would probably be convenient if E_0 were selected as 1 Mev and the resonance region assumed to end at this energy. (In most cases, very little error would result in doing this.)

If the limits are taken in ascending order of energy, the A_i's or all the integrals should be multiplied by a negative sign. The reason for this is that lethargy decreases as energy increases.

Since the resonance type foils are most applicable for the determination of differential flux, the integral matrix would not be used. The correct u_i's should be more easily determined than in the threshold detector situation, for the resonance cross sections are quite sharply

peaked. If the α_i's are large, the u_i's should be the lethargies corresponding to the maximum cross section values; if the α_i's are small, the u_i's will be somewhat different.

The polygonal method is not presently suitable for use in the resonance region because of the lack of data regarding the true cross sections of suitable materials. However, it is hoped that a test calculation involving hypothetical cross sections can be made in the near future. The results of this calculation should give an indication of the validity of the polygonal method when applied to the 1/E spectral region.

VI. The Polynomial Method

Basic Philosophy

The basic postulate of the polynomial method is that the differential flux can be represented by a polynomial, the degree of which is one less than the number of detectors used. It is well known that any function can be represented by an infinite series; however, when this series is reduced to a polynomial, large errors can occur in the representation. In order that representation errors be reduced, the infinite series must be rapidly converging over the interval. If this is the case, the first few terms of the series will be sufficient for fairly accurate representation of the true function.

Application to Threshold Type Foils

General Equations in Energy Space. The assumption is made that the following expansion is possible*:

$$\phi(E) = \phi_0(E) \left[a_0 + a_1 E + a_2 E^2 + \cdots a_{N-1} E^{N-1} \right] \qquad (46)$$

* If one of the foils (such as plutonium) has an appreciable cross section in the region of 1/E spectral dominance, the following equation should be used in place of Eq. (46);

$$\phi(E) = a_0/E + \phi_0(E) \left[a_1 + a_2 E + a_3 E^2 + \cdots a_{N-1} E^{N-2} \right] \qquad (46A$$

The representation of Eq. (46) is not satisfactory because the fission spectrum decreases at low energies whereas the 1/E spectrum increases.

Where: N is the number of different detectors used.

$\phi_o(E)$ is the normalized fission spectrum.

The activities, A_i's, are written as follows:

$$A_i = \int_o^\infty \phi(E)\ \sigma_i(E)\ dE = \int_o^\infty \phi_o(E)\left[a_o + a_1 E + \cdots\right]\ \sigma_i(E)\ dE \qquad (47)$$

Expanding:

$$A_i = a_o \int_o^\infty \phi_o(E)\ \sigma_i(E)\ dE + a_1 \int_o^\infty \phi_o(E)\ E\ \sigma_i(E)\ dE +$$

$$a_2 \int_o^\infty \phi_o(E)\ E^2\ \sigma_i(E)\ dE + \cdots \qquad (48)$$

In order that a digital computer can easily handle the required calculation, the following change in the equations is made:

(1) X is substituted for E/10.

(2) $\int_{14\ Mev}^{\infty} \phi_o(E)\ dE$ is set equal to zero --- an approximation.

Now, A_i becomes the following:

$$A_i = a_o \int_o^{14} \phi_o(X)\ \sigma_i(X)\ dX + a_1 \int_o^{14} \phi_o(X)\ X\ \sigma_i(X)\ dX + \cdots \qquad (49)$$

where $\phi(X) = 10\ \phi_o(E)$

and $\phi(X) = \phi_o(X)\left[a_0 + a_1 X + a_2 x^2 + \cdots a_{N-1} X^{N-1}\right]$

For N foils, each with relatively "independent" cross sectional derivatives, the following matrix equation can be generated:

$$(A) = (C)\,(a) \qquad (50)$$

Where (C) is the matrix of the calculated integrals; that is:

$$C_{11} = \int_0^{1.4} \phi_o(x)\ \sigma_1(x)\ dx$$

$$C_{22} = \int_0^{1.4} x\ \phi_o(x)\ \sigma_1(x)\ dx$$

$$C_{ij} = \int_0^{1.4} x^{j-1}\ \phi_o(x)\ \sigma_i(x)\ dx$$

$$C_{NN} = \int_0^{1.4} x^{N-1}\ \phi_o(x)\ \sigma_N(x)\ dx$$

Solving the matrix equation for (a):

$$(a) = (C)^{-1}\,(A) \qquad (51)$$

Determining the a_j's by this method, $\phi(X)$, and therefore $\phi(E)$, can be theoretically found for any E or X.

Recalling that threshold type detectors are best suited for integral measurements, the following technique should be used:

$$\text{Let: } \left(\Phi(x)\right)_j = (I)\,(a) \qquad (52)$$

where (I) is the integral matrix depending upon X.

Now:

$$(I)\ (a) = (I)\ (C)^{-1}\ (A) = \left(\mathcal{F}(X)\right) \tag{53}$$

The determination of which energy values to use in the integration is done as follows:

1. Several X values are selected and the following integration vector is computed for each X. (This integration vector is one row of the integration matrix.) The X values are selected from the effective threshold energy regions.

$$(\bar{J}) = \left(\int_{x'}^{1.4} \phi_o(x)\,dx \quad \int_{x'}^{1.4} \phi_o(x)\,x\,dx \quad \cdots \quad \int_{x'}^{1.4} \phi_o(x)\,x^{N-1}\,dx \right) \tag{54}$$

Upon completion of the above computation, each integration vector $(\bar{J})$ is multiplied by $(C)^{-1}$ to form $(\bar{J})\ (C)^{-1}$.

For one particular X, the resulting vector will most closely approach one of the following forms:

1. $\left(k_1 \quad m_{12} \quad m_{13} \cdots m_{1j} \cdots \right)$

2. $\left(m_{21} \quad k_2 \quad m_{23} \cdots \cdots \cdots \right)$

3. $\left(m_{31} \quad m_{32} \quad k_3 \cdots \cdots \cdots \right)$

where the K_i of each vector is maximized with respect to the m_{ij}'s.

Form 1 is approximated when X values corresponding to the first (A_1) detector are used; Form 2 is approximated when X values corresponding to the second detector (A_2) are used, etc.

By this procedure, one determines the E_j which leads to the best vector. The best vector is the vector which gives the minimum error for an error in the activation. These vectors are then used to generate a square matrix, the ideal form of such a matrix being the following:

$$(k) = \begin{pmatrix} k_1 & — & — & — & — \\ — & k_2 & — & — & — \\ — & — & k_3 & — & — \\ \cdots & \cdots & \cdots & \cdots & — \\ — & — & — & — & k_N \end{pmatrix} \qquad (55)$$

Taking the product of this matrix and the A_i matrix gives N values for $\underline{\Phi}(X)$. In this manner, it is believed that the best integral flux information is generated.

$$(\underline{\Phi}(X)) = (k)(A) \qquad (56)$$

For the ideal case:

$$\Phi_1 = k_1 A_1 = \int_{X_1}^{1.4} \phi(x)\, dx$$

$$\Phi_N = k_N A_N = \int_{X_N}^{1.4} \phi(x)\, dx \qquad (57)$$

Which is the formulism of the Trice Method; however, in this case the true cross sections have been used, and the assumptions regarding the spectrum have been less constraining.

General Equations in Gay Space. The polynomial used in energy space was selected almost arbitrarily; however, some types of polynomials should be better than others when applied to the neutron spectra problem. A theoretical method of selecting a "best" polynomial is not known by the author; however, a polynomial in gay space seems to have some advantages. Let such a polynomial be represented by the following:

$$\phi(g) = a_0 + a_1 g + a_2 g^2 + \cdots a_{N-1} g^{N-1} \qquad (58)$$

As in energy space, only the a_0 will be non-zero if the real spectrum is a fission spectrum; however, in gay space the anticipated spectrum is more properly weighted, for the flux-spectrum assumes more importance at low energies than at high ones.

A practical advantage in using the polynomial method in gay space is that the calculations are greatly simplified. The loss of the $\phi_o(E)$ weighting factor, particularly in the integration vector, is responsible for this simplification.

The procedure for using gay rather than energy in the polynomial calculations is the same as before, with one exception --- $\phi_o(E)$ is no longer used.

An example of this change follows:

$$A_i = a_0 \int_0^{1.0} \sigma_i(g)\, dg + a_1 \int_0^{1.0} g\, \sigma_i(g)\, dg + \cdots \tag{59}$$

$$C_{11} = \int_0^{1.0} \sigma_1(g)\, dg \tag{60}$$

The integration vector, $\bar{J}$, becomes the following:

$$(\bar{J}) = (g \quad g^2/2 \quad g^3/3 \cdots g^N/N) \tag{61}$$

(This can be simply calculated by hand for many values of g.)

Once the cross sections as a function of gay are computed, the remainder of the calculation can be made in a simple manner. In calculating the cross sections, care must be taken with materials having high-energy thresholds, for the gay intervals, as compared with those of energy, are very small in the high energy region.

By forming a matrix of the best $(\bar{J})(C)^{-1}$ vectors, the happy flux is obtained, as before, by multiplication with the activity matrix. The happy flux can be easily transformed to energy flux by simple conversion of gay to energy, for the following quality is true by definition:

$$\underline{\Phi}(g) = \underline{\Phi}(E), \tag{62}$$

where g and E correspond.

This method has not yet been tested using materials having sufficient independency in their cross sectional derivatives. It has been found that very poor results will be obtained if two of the cross sectional derivatives are quite dependent; i.e., sulfur-32 and phosphor-31. (The $\Phi(g)$ matrix becomes very poorly conditioned.)

Application to Resonance Type Detectors

In the resonance region it seems plausible that a polynomial in lethargy could be used. A possible polynomial is the following:

$$\phi(u) = a_0 + a_1 u + a_2 u^2 + \cdots a_{N-1} u^{N-1} \qquad (63)$$

Using the procedures described in the previous subsection, a matrix equation for the A_i's can be found.

$$(a) = (C)^{-1} (A) \qquad (64)$$

The A_i's calculated in the foregoing manner are the coefficients of the lethargy flux polynomial; hence, in theory the lethargy flux becomes known for all lethargies. Practically, this is probably not true, for the polynomial will most likely represent the true lethargy flux at N lethargies only.

Each of the N lethargies should be selected by the same method as described previously for the threshold type foils. Once the proper ϕ_j's are determined, the approximate lethargy flux throughout the 1/E interval can be obtained by constructing a smooth curve through the ϕ_j points.

VII. Numerical Results of Test Case Using Polynomial Method in Energy Space

As an indicator of usefulness for practical work, a test case for the polynomial method is presented in this section.

The test is made using the following spectra:

1. $\phi(E) = .0715$ per Mev for all E less than 14 Mev.
   $\phi(E) = 0$ for all E greater than 14 Mev. (8)
2. $\phi(E) = .38/E$ per Mev for E greater than 1 Mev and less than 14 Mev.
   $\phi(E) = .38$ per Mev for E greater than 0 Mev and less than 1 Mev.
   $\phi(E) = 0$ for E greater than 14 Mev. (9)
3. $\phi(E) = .0102(14-E)$ per Mev for E greater than 0 Mev and less than 14 Mev.
   $\phi(E) = 0$ for E greater than 14 Mev. (10)
4. $\phi(E) = .454e^{-E/.965} \sinh \sqrt{2.29E}$ per Mev for all E.
   (The California fission spectrum.)

The materials and specific reactions used are as follows:

$$Np^{237}(n,f) \longrightarrow \sigma_1$$

$$U^{238}(n,f) \longrightarrow \sigma_2$$

$$S^{32}(n,p)P^{32} \longrightarrow \sigma_3$$

$$Si^{28}(n,p)Al^{28} \longrightarrow \sigma_4$$

$$Al^{27}(n,\alpha)Na^{24} \longrightarrow \sigma_5$$

These materials are the most independent of the group of seven found in Appendix B.

The (C) matrix, as calculated by the Wright Air Development Center Univac-1103, is as follows:

$$\begin{pmatrix} 1178.6 & 289.18 & 103.15 & 49.727 & 30.021 \\ 292.28 & 88.390 & 32.836 & 15.051 & 8.3735 \\ 64.551 & 26.782 & 12.689 & 6.8942 & 4.2864 \\ 4.5385 & 3.3009 & 2.491 & 1.9579 & 1.6059 \\ .38225 & .35128 & 3.314 & .3211 & .31925 \end{pmatrix}$$

The inverse (C) matrix, $(C)^{-1}$, is as follows:

$$\begin{pmatrix} .009345 & -.05221 & .09593 & -.2460 & .4400 \\ -.09481 & .6725 & -1.551 & 4.090 & -8.467 \\ .03085 & -2.464 & 6.658 & -20.11 & 47.37 \\ -.3889 & 3.315 & -9.802 & 34.85 & -94.07 \\ .1640 & -1.453 & 4.538 & -18.38 & 57.35 \end{pmatrix}$$

(J) $(C)^{-1}$ vectors for several energies are as follows:

E	$\bar{JC}_1$	$\bar{JC}_2$	$\bar{JC}_3$	$\bar{JC}_4$	$\bar{JC}_5$
*.6	7.569×10^{-4}	-6.979×10^{-5}	-3.868×10^{-4}	-2.561×10^{-3}	-3.398×10^{-3}
.7	6.001×10^{-4}	5.755×10^{-4}	-1.127×10^{-3}	-5.552×10^{-4}	-5.734×10^{-3}
.8	4.633×10^{-4}	1.089×10^{-3}	-1.599×10^{-3}	8.268×10^{-4}	-6.955×10^{-3}
1.2	1.011×10^{-4}	2.025×10^{-3}	-1.443×10^{-3}	1.822×10^{-3}	-4.582×10^{-3}
*1.4	7.999×10^{-6}	2.008×10^{-3}	-6.072×10^{-4}	7.821×10^{-4}	-1.452×10^{-3}
1.6	-4.313×10^{-5}	1.800×10^{-3}	4.275×10^{-4}	-5.657×10^{-4}	1.621×10^{-3}
*2.8	-2.282×10^{-6}	-1.443×10^{-4}	4.571×10^{-3}	-2.732×10^{-3}	2.031×10^{-3}
3.0	1.327×10^{-5}	-3.259×10^{-4}	4.605×10^{-3}	-1.836×10^{-3}	-2.753×10^{-4}
5.0	2.177×10^{-5}	-2.434×10^{-4}	1.092×10^{-3}	6.746×10^{-3}	-1.077×10^{-2}
5.2	1.669×10^{-5}	-1.828×10^{-4}	7.899×10^{-4}	6.821×10^{-3}	-9.690×10^{-3}
*5.4	1.193×10^{-5}	-1.278×10^{-4}	5.302×10^{-4}	6.752×10^{-3}	-8.352×10^{-3}
8.0	-3.898×10^{-6}	3.923×10^{-5}	-1.472×10^{-4}	9.354×10^{-4}	9.493×10^{-3}
8.2	-3.033×10^{-6}	3.015×10^{-5}	-1.108×10^{-4}	5.685×10^{-4}	9.983×10^{-3}
*8.4	-2.131×10^{-6}	2.082×10^{-5}	-7.414×10^{-5}	2.401×10^{-4}	1.033×10^{-2}

The starred notation indicates the best vectors to use. The selection method used is described on page 50. It should be noted that certain dependencies and poor selections of energy values exist. The best vectors are summarized by the following:

.6 Mev < E_1 < .65 Mev.

1.4 Mev < E_2 < 1.5 Mev.

2.1 Mev < E_3 < 3.0 Mev, dependence with U-238 and Si-28 is indicated.

5.4 Mev < E_4, lack of evidence regarding dependence (should find dependence with S-32).

8.4 Mev < E_5, again with lack of evidence regarding dependence.

The notation used above indicates the energy range in which the best E_j should be found. The vectors can be optimized by performing further calculations within the energy intervals. It is noted that the E_4 and E_5 guesses were quite in error.

As an aid in visualizing the qualitative differences between the vectors, the vectors can be multiplied by the first row of the (C) matrix (this generates the flux equation for a normalized fission spectrum). The following vector array has been computed in this manner.

E (Mev)	$(\bar{J})\ (C)^{-1}\ (A)$				
* .6	.890	-.02	-.025	-.0116	-.00130
.7	.705	.168	-.072	-.0025	-.00219
1.2	.119	.591	-.0934	.00825	-.00175
* 1.4	.00942	.585	-.0388	.00354	-.000555
1.6	-.0508	.526	.0277	-.00256	.000616

E (Mev)	$\bar{\bar{J}}$ (C)$^{-1}$ (A)				
* 2.8	-.00268	-.0421	.296	-.01235	.000776
3.0	.0156	-.095	.297	-.00830	-.000105
5.0	.0256	-.071	.0704	.0304	-.00412
5.2	.0196	-.0531	.0510	.0308	-.0037
* 5.4	.0141	-.0371	.0342	.0306	-.00319
8.0	-.00457	.01145	-.0095	.00424	.0362
8.2	-.00356	.0088	-.00715	.00256	.00381
* 8.4	-.00251	.00606	-.00479	.00108	.00394

From the preceding array, the best E_j's can be selected (the starred values).

By taking the sum of the elements in each row, the fission spectrum integral flux for the particular E_j's can be found. The results of this addition are as follows:

E (Mev)	$\oint$(E) calculated	$\oint$(E) true
.6	.832	.835
.7	.796	.799
1.2	.623	.625
1.4	.559	.560
1.6	.500	.501

E (Mev)	Φ(E) calculated	Φ(E) true
2.8	.240	.239
3.0	.209	.209
5.0	.0513	.0515
5.2	.0446	.0444
5.4	.0386	.0383
8.0	.00524	.00521
8.2	.00446	.00445
8.4	.00378	.00379

It is believed that the results can be considered as satisfactory.

Figures 10 and 11 are the graphical results of the test calculation mentioned earlier in this section. The activities used were numerically calculated by using the test spectrum and the true cross sections. The (J) $(C)^{-1}$ vectors used were those corresponding to E_j's of 0.6, 1.4, 2.8, 5.4, and 8.4 Mev. Worse results were expected from the 5.4 and 8.4 Mev calculations than what actually occurred.

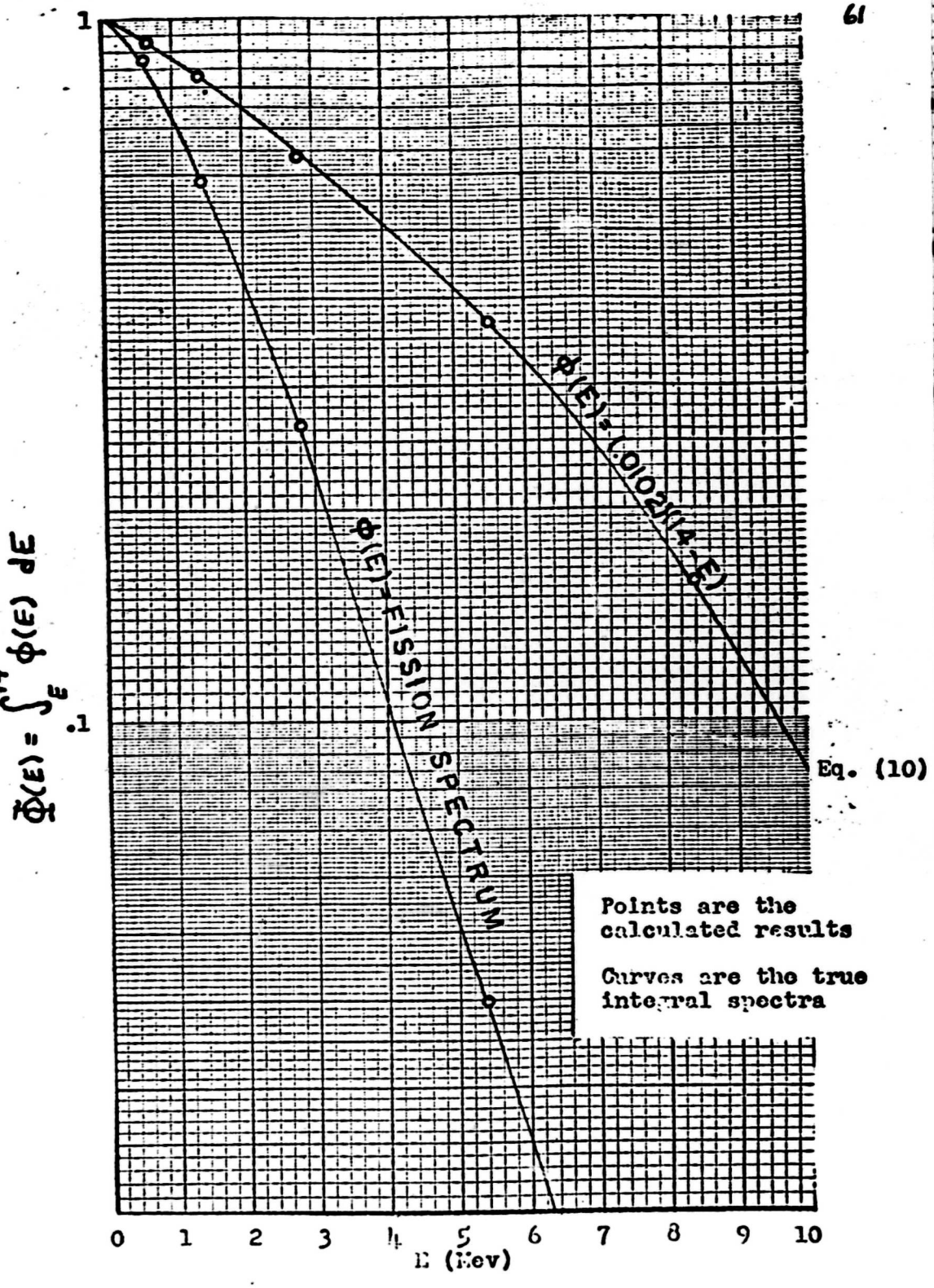

Figure 10

Prediction of Spectra by the Polynomial Method

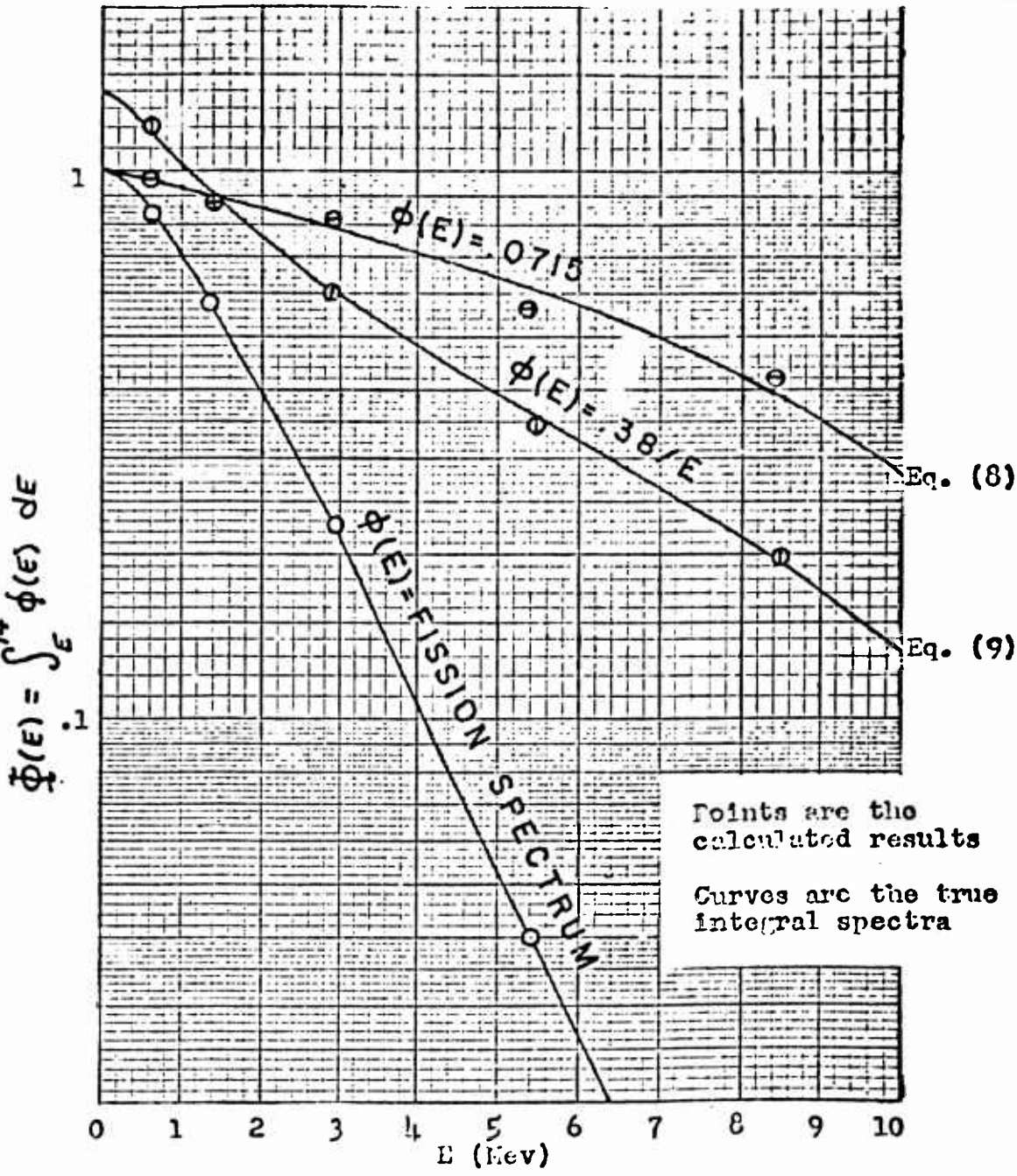

Figure 11

Prediction of Spectra by the Polynomial Method

VIII. Conclusions

Several methods for obtaining neutron flux-spectra information have been presented. The simplest of these is the Trice Method; however, this method is also the most inaccurate. Where the Trice fast-neutron method gives results accurate to ± 50% for various spectra, the polynomial method in energy space reduces this error to ± 10% even when the polynomial integral matrix is not optimized. (See the Trice method and polynomial test case results.) The polynomial method, optimized in gay space, should give even better results. On the other hand, if the available cross sections are not suitably orthogonal, the Trice methods are the most useable.

The most difficult method to work with is the polygonal method, for E_j selections must be made before the (C) matrix can be calculated.

It is hoped that the results of the polynomial optimization can be published in the near future.

Bibliography

1. Cranberg, L. "Fission Neutron Spectrum of U-235." Physical Review, 103: 662-670 (1 August 1956).

2. Goldstein, N., et al. Argonne National Laboratory Quarterly Report. CF-3574. 1946.

3. Hughes, D. J. and J.A. Harvey. Neutron Cross Sections. BNL 325. Washington: GPO, 1955.

4. Hughes, D. J. Pile Neutron Research. Cambridge, Mass: Addison-Wesley Publishing Co., 1953.

5. Hurst, G. S., et al. Neutron Flux and Tissue Dose Studies with Fission Threshold Detectors. ORNL 1671. Secret, Restricted Data. 1954.

6. Hurst, G. S., et al. "Techniques of Measuring Neutron Spectra with Threshold Detectors - Tissue Dose Determination." The Review of Scientific Instruments. 27: 153-156. (March 1956).

7. Klema, E. D., and A. O. Hanson, "A Determination of the $S^{32}(n,p)P^{32}$ Cross Section for Neutrons Having Energies of 1.6 to 5.8 Mev." Physical Review, 73: 106. (15 January 1948).

8. Macklin, R. L., and H. S. Pomerance. "Resonance Capture Integrals." Proceedings of the International Conference on the Peaceful Uses of Atomic Energy. 5: 96-101. (1956).

9. Marion, J. B., et al. "Cross Section for the $Si^{28}(n,p)Al^{28}$ Reaction." Physical Review, 101: 247-249. (1 January 1956).

10. Trice, J. B., et al. A Series of Thermal Epithermal and Fast Neutron Measurements in the MTR. ORNL-CF-55-10-240. Oak Ridge, Tenn: Oak Ridge National Laboratory. 1955.

11. Trice, J. B. Fast Neutron Flux Measurements in E-25 of the Brookhaven Graphite Reactor. ORNL-CF-55-7-130. Oak Ridge, Tenn: Oak Ridge National Laboratory. 1955.

12. Segre, E. G. Experimental Nuclear Physics. New York: John Wiley Publishing Co. 1953.

13. Watt, B. E. Energy Spectrum of Neutrons from Fissions Induced by Thermal Neutrons. LA-718. Los Alamos, N. M.: Los Alamos Scientific Lab. 1948.

Appendix A

The Calculation of First-Collision Energy Absorption from Spectral Data

The first-collision dose rate in a material undergoing irradiation can be approximately calculated from the following:

$$D(E_j) = \frac{1-\alpha}{2} \int_{E_j}^{\infty} E\, N\, \sigma_s(E)\, \phi(E)\, dE \quad \frac{Mev}{cc.\,sec.}$$

Where: $\alpha = \left(\frac{A-1}{A+1}\right)^2$, A being the mass number of the material.

$N\sigma_s(E)$ = macroscopic scattering cross section of the irradiated material.

E = neutron energy in Mev.

$\phi(E)$ = differential neutron flux in neutrons/cm^2-sec-Mev.

$D(E_j)$ = dose contributed by neutrons of energy E_j and greater.

Knowing $\phi(E)$, the dose rate can be calculated. Under some circumstances only values of $\int_{E_j}^{\infty} \phi(E)\, dE$ are available. If the scattering cross section is approximately constant, the dose can be calculated as follows:

$$D(E_j) = \frac{1-\lambda}{2} \int_{E_j}^{\infty} E\, \Sigma_s(E)\, \phi(E)\, dE = \frac{1-\lambda}{2} \Sigma_s \int_{E_j}^{\infty} E\, \phi(E)\, dE$$

Integrating by parts with $u = E$, $du = dE$, $dv = \phi(E)\, dE$ $v = \int_0^E \phi(E')\, dE'$:

$$D(E_j) = \frac{1-\lambda}{2} \Sigma_s \left\{ \left[E \left\{ \Phi_0 - \Phi(E) \right\} \right] \Big|_{E_j}^{\infty} - \int_{E_j}^{\infty} \left[\Phi_0 - \Phi(E) \right] dE \right\}$$

where:

$$\Phi_0 = \int_0^{\infty} \phi(E)\, dE$$

$$\Phi(E) = \int_E^{\infty} \phi(E')\, dE'$$

$$\int_0^E \phi(E')\, dE' = \int_0^{\infty} \phi(E')\, dE' - \int_E^{\infty} \phi(E')\, dE' = \Phi_0 - \Phi(E)$$

After substitution of limits, the following is obtained:

$$D(E_j) = \frac{1-\lambda}{2} \Sigma_s \left[E_j\, \Phi(E_j) + \int_{E_j}^{\infty} \Phi(E)\, dE \right]$$

If $\Phi(E)$ is known, the dose received in any energy interval can be obtained.

For an energy dependent scattering cross section, the following formula can be used:

$$D(E_j) = \frac{1-A}{2}\left\{ 14\,\Sigma_s(14)\,\Phi_0 - \Sigma_s(E_j)\,E_j\,\phi_0 + \Sigma_s(E_j)\,E_j\,\Phi(E_j) \right.$$

$$\left. - \int_{E_j}^{14} E\,\frac{d\Sigma_s(E)}{dE}\left[\Phi_0 - \Phi(E)\right]dE - \int_{E_j}^{14} \Sigma_s(E)\left[\phi_0 - \Phi(E)\right]dE \right\}$$

where it has been assumed that $\int_{14}^{\infty} \phi(E)\,dE = 0$

The derivation of the above formula was made in the same manner as that for the constant scattering cross section.

Appendix B

Compilation of (n,p), (n,d), and (n,f) Cross Sections

The following is a tabulation of cross sections for several threshold and fast-fission type detectors. In many cases the cross-sections have been "smoothed" for reasons of calculational convenience. The sources of data are the same as those listed in Table 1.

Key

σ_1 ——— $Np^{237}(n,f)$

σ_2 ——— $U^{238}(n,f)$

σ_3 ——— $P^{31}(n,p)Si^{31}$

σ_4 ——— $S^{32}(n,p)P^{32}$

σ_5 ——— $Al^{27}(n,p)Mg^{27}$

σ_6 ——— $Si^{28}(n,p)Al^{28}$

σ_7 ——— $Al^{27}(n,d)Na^{24}$

σ_i ——— Units of 10^{-3} barns(mb)

E ——— Units of Mev

E	σ_1	σ_2	σ_3	σ_4	σ_5	σ_6	σ_7
0.1	0	0	0	0	0	0	0
0.2	25						
0.3	66						
0.4	165						
0.5	390						
0.6	640	0					
0.7	900	1.5					
0.8	1060	3					
0.9	1180	11					
1.0	1250	15					
1.2	1350	46					
1.4	1370	150					
1.6	1400	410	0	0			
1.8	1400	490	5	15			
2.0	1420	530	10	25			
2.2	1450	540	28	50			
2.4	1450	550	35	80			
2.6	1450	550	50	80			
2.8	1450		60	100	0		
3.0	1450		54	130	1		
3.2	1460		71	165	2		
3.4	1470	550	68	220	4		

E	σ_1	σ_2	σ_3	σ_4	σ_5	σ_6	σ_7
3.6	1470	550	71	225	6	0	0
3.8	1480		80	215	6		
4.0	1490		80	230	7		
4.2	1490		80	260	8		
4.4	1490		80	265	10		
4.6	1490		80	265	16		
4.8	1460		80	270	18	0	
5.0	1450		79	275	20	10	
5.2	1450		79	280	25	14	
5.4	1450		79	280	27	27	
5.6	1500		79	285	32	33	
5.8	1600		79	285	36	44	
6.0	1700		79	290	40	60	
6.2	1800		79	295	44	77	0
6.4	1900		79	295	48	110	1
6.6	2000		79	300	51	140	3
6.8	2150		79	300	55	150	4
7.0	2250		79	305	60	170	5
7.2	2300		79	310	62	180	7
7.4	2400		79	312	70	190	9
7.6	2450		79	315	74	190	13
7.8	2500		79	318	76	200	17
8.0	2525	550	78	320	78	210	21

E	σ_1	σ_2	σ_3	σ_4	σ_5	σ_6	σ_7
8.2	2550	550	78	322	79	220	26
8.4	2550			324	80		32
8.6	2550			326			37
8.8	2560			320			51
9.2	2600			332			58
9.4	2600			334			67
9.6				336			75
9.8				338			86
10.0				340			93
11				350			110
12				360			110
13				365			110
14	2600	550	78	370	80	220	110

Appendix C

The Normalized Watt and California Fission Spectra

The following is a table of ordinates and integrals for two commonly used uranium-235 fission spectra functions. The functions have been normalized such that $\int_0^\infty \phi_w(E)\,dE = 1$ and $\int_0^{14} \phi_c(E)\,dE = 1$.

$$\phi_w(E) = .483\, e^{-E} \sinh \sqrt{2E} = \text{The Watt Spectrum} \quad [13]$$

$$\phi_c(E) = .454\, e^{-E/.965} \sinh \sqrt{2.29E} = \text{The University of California Spectrum} \quad [1]$$

where: E is the neutron energy in Mev.

The Watt Spectrum

E_j(Mev)	$\phi_w(E)$	$\int_0^{E_j} \phi_w(E)dE$	$\int_{E_j}^{\infty} \phi_w(E)dE = \Phi_w(E)$
0.1	.202	.0140	.9860
0.2	.267	.0377	.9623
0.3	.306	.0663	.9337
0.4	.330	.0987	.9013
0.5	.345	.1321	.8679

E_j(Mev)	$\phi_w(E)$	$\int_0^{E_j} \phi_w(E)dE$	$\int_{E_j}^{\infty} \phi_w(E)dE = \xi_w(\varepsilon)$
0.6	.352	.1669	.8331
0.7	.355	.2027	.7973
0.8	.354	.2385	.7615
0.9	.351	.2729	.7271
1.0	.344	.3082	.6918
1.1	.337	.3425	.6575
1.2	.327	.3759	.6241
1.3	.318	.4074	.5926
1.4	.307	.4383	.5617
1.6	.284	.4983	.5017
1.8	.260	.5631	.4369
2.0	.237	.6028	.3972
2.5	.184	.7073	.2927
3.0	.138	.7876	.2124
3.5	.1025	.8476	.1524
4.0	.0748	.8914	.1086
4.5	.0538	.9192	.0808
5.0	.0384	.9463	.0537
5.5	.0272	.9624	.0376
6.0	.0191	.9739	.0261

E_j(Mev)	$\phi_w(E)$	$\int_0^{E_j} \phi_w(E)dE$	$\Phi_w(E_j)$
6.5	.0133	.9321	.0179
7.0	9.31×10^{-3}	.9876	.0124
7.5	6.43×10^{-3}	.9916	.0084
8.0	4.42×10^{-3}	.9943	.0057
8.5	3.04×10^{-3}	.9960	.0040
9.0	2.07×10^{-3}	.9973	.0027
9.5	1.42×10^{-3}	.9982	.0018
10.0	9.53×10^{-4}	.9987	1.21×10^{-3}
11.	4.38×10^{-4}	.9994	5.50×10^{-4}
12.	1.99×10^{-4}	.9997	2.47×10^{-4}
13.	8.95×10^{-5}	.9999	1.10×10^{-4}
14.	4.00×10^{-5}	.99995	4.87×10^{-5}

The California Spectrum

E_j(Mev)	$\phi_c(E)$	$\int_o^E \phi_c(E)dE$	$\int_{E_j}^{14} \phi_c(E)dE \equiv \Phi_c(E_j)$
.1	.203	.0102	.989
.2	.269	.0338	.965
.3	.308	.0624	.936
.4	.330	.096	.904
.5	.348	.130	.870
.6	.355	.165	.835
.7	.360	.201	.799
.8	.357	.237	.763
.9	.351	.272	.728
1.0	.346	.307	.693
1.1	.341	.341	.659
1.2	.331	.375	.625
1.3	.322	.408	.592
1.4	.309	.440	.560
1.5	.297	.470	.530
1.6	.285	.499	.501
1.8	.263	.554	.446
2.0	.239	.604	.396

E_j(Mev)	$\phi_c(E)$	$\int_0^{E_j} \phi_c(\varepsilon)\, d\varepsilon$	$\Phi_c(E_j)$
2.2	.218	.650	.350
2.4	.196	.691	.309
2.6	.175	.728	.272
2.8	.156	.761	.239
3.0	.138	.791	.209
3.2	.123	.817	.183
3.4	.109	.840	.160
3.6	.0956	.861	.139
3.8	.0840	.879	.121
4.0	.0742	.894	.106
4.2	.0660	.9084	.0916
4.4	.0564	.9206	.0794
4.6	.0491	.9312	.0688
4.8	.0435	.9404	.0596
5.0	.0375	.9485	.0515
5.2	.0326	.9556	.0444
5.4	.0284	.9617	.0383
5.6	.0246	.9670	.0330
5.8	.0214	.9716	.0284
6.0	.0184	.9755	.0245

E_j (Mev)	$\phi_c(E)$	$\int_0^{E_j} \phi_c(E)dE$	$\Phi_c(E_j)$
6.2	.0159	.9790	.0210
6.4	.0138	.9819	.0181
6.6	.0119	.9845	.0155
6.8	.0102	.9867	.0133
7.0	8.80×10^{-3}	.9886	.0114
7.2	7.58×10^{-3}	.9903	9.75×10^{-3}
7.4	6.52×10^{-3}	.9917	8.34×10^{-3}
7.6	5.55×10^{-3}	.9929	7.13×10^{-3}
7.8	4.83×10^{-3}	.9939	6.09×10^{-3}
8.0	4.11×10^{-3}	.9947	5.21×10^{-3}
8.2	3.50×10^{-3}	.9956	4.45×10^{-3}
8.4	3.07×10^{-3}	.9962	3.79×10^{-3}
8.6	2.60×10^{-3}	.9968	3.22×10^{-3}
8.8	2.21×10^{-3}	.9978	2.74×10^{-3}
9.0	1.89×10^{-3}	.9981	2.33×10^{-3}
9.5	1.26×10^{-3}	.9987	1.54×10^{-3}
10.0	8.30×10^{-4}	.9992	1.02×10^{-3}
10.5	5.62×10^{-4}	.9994	6.69×10^{-4}
11.0	3.83×10^{-4}	.9996	4.33×10^{-4}

E_j (Mev)	$\phi_c(E)$	$\int_0^{E_j} \phi_c(E)dE$	$\Phi_c(E_j)$
11.5	2.61×10^{-4}	.9997	2.72×10^{-4}
12.0	1.76×10^{-4}	.9998	1.625×10^{-4}
12.5	1.08×10^{-4}	.9999	9.15×10^{-5}
13.0	7.30×10^{-5}	.9999	5.12×10^{-5}
13.5	4.91×10^{-5}	.9999	2.07×10^{-5}
14.0	3.32×10^{-5}	1.0000	- - - - -

Appendix D

The Derivation of an Activation Identity

It is the purpose of this appendix to derive the following relationship:

$$A = \int_0^\infty \sigma(E)\,\phi(E)\,dE \equiv \int_0^\infty \bar{\Phi}(E)\,\frac{d\sigma}{dE}\,dE$$

Where: A = the activation function.

$\sigma(E)$ = the activation cross section as a function of energy---threshold type foil.

$\phi(E)$ = the differential neutron flux.

E = the neutron energy

$\bar{\Phi}(E) = \int_E^\infty \phi(E')\,dE'$ = the integral flux

Integrating the first integral by parts,

$$A = \sigma(E)\left[\bar{\Phi}(0) - \bar{\Phi}(E)\right]\Big|_0^\infty - \int_0^\infty \left[\bar{\Phi}(0) - \bar{\Phi}(E)\right]\frac{d\sigma(E)}{dE}\,dE$$

Where: $\bar{\Phi}(0) = \int_0^\infty \phi(E)\,dE$

$\bar{\Phi}(E) = \int_E^\infty \phi(E')\,dE'$

Noting that $\bar{\Phi}(\infty) = 0$, and $\sigma(0) = 0$,

$$A = \int_0^\infty \bar{\Phi}(E)\,\frac{d\sigma}{dE}\,dE$$

Therefore,

$$\int_0^\infty \phi(E)\,\sigma(E)\,dE \equiv \int_0^\infty \bar{\Phi}(E)\,\frac{d\sigma}{dE}\,dE$$

Appendix E

Activation Shielding with Boron

One practical solution to the α problem discussed on page 31 may be to cover seach foil with a sufficient quantity of boron. Boron has an almost pure 1/v cross section for activation.

Using a boron covering results in a reduction of the number of low energy neutrons traversing the foil. Such a situation could be responsible for improving results, for the apparent α's are increased.

$$\alpha = \frac{\text{activation due to resonance cross section}}{\text{activation due to 1/v cross section}}$$

The activation shielding with boron can be calculated from the following:

$$A = \int_0^\infty e^{-\Sigma_{2200}\sqrt{\frac{.025}{E}}\,\bar{t}}\ \sigma(E)\ \phi(E)\ dE$$

Where: $e^{-\Sigma_{2200}\sqrt{\frac{.025}{E}}\,\bar{t}}$ = the boron transmission factor.

$\Sigma_{2200} = N\sigma_{2200}$ = the boron macroscopic absorption cross section at 2200 m/sec neutron velocity.

E = the neutron energy in ev.

$\bar{t}$ = the effective thickness of the boron cover. (approximately 2 times the true thickness in an isotropic flux).

$\sigma(E)$ = the activation cross section of the resonance detector.

$\phi(E)$ = the differential neutron flux.

The above equation can be written as follows:

$$A = \int_0^\infty T(E)\left\{(\sigma - \sigma_{res}) + \sigma_{res}\right\}\phi(E)\,dE$$

$$\simeq T(E_o)\int_{\Delta E}\sigma_{res}\,\phi(E)\,dE + \int_0^{100\ ev} T(E)\,\sigma\,\phi(E)\,dE$$

$$\simeq \phi_o\,T(E_o)\int_{\Delta E}\sigma_{res}\,dE/E + \int_0^{100\ ev} T(E)\,\sigma\,\phi(E)\,dE$$

Where: T(E) = the transmission factor previously defined.

σ = the total activation cross section, as a function of energy, of the resonance detector.

σ_{res} = the resonance cross section, as a function of energy, of the resonance detector.

E_o) = the value of the transmission factor at the energy of the resonance.

ϕ_o = the neutron flux per unit lethargy.

If the second integral of the preceding equation is negligible compared with the first, an opportunity for determining ϕ_o exists. The second term is made suitably small by proper slection of $\bar{t}$. Thirty thermal neutron relaxation lengths should be sufficient; therefore,

$\bar{t}$ should be approximately .05 inches. To insure that thermal neutron protection is present, a small thickness of cadmium should be placed between the boron and the detector.

GNE-9

Vita

The author of this thesis, First Lieutenant Paul M. Uthe, Jr., [redacted] He is the son of Mrs. Kota [redacted] of Hatton, North Dakota, and Mr. Paul M. Uthe of Watertown, South Dakota. Lt. Uthe attended high school at Watertown, South Dakota, and college at the South Dakota State College, Brookings, South Dakota, where he received a degree of Bachelor of Science in Engineering Physics in June 1952. He attended the Air force Institute of Technology, Wright-Patterson AFB, Ohio from September 1955 to March 1957 at which time he graduated with a Master of Science degree in Nuclear Engineering.

[redacted]

This thesis was typed by S/Sgt. H. L. Lister.